UNIVERSITY OF WISCONSIN-LA CROSSE

Graduate Studies

MORPHOLOGICAL RESPONSES TO SK-03-92 IN EUKARYOTIC CELLS

A Manuscript Style Thesis Submitted in Partial Fulfillment of the Requirements for the Degree of Master of Science

Timothy J Green

College of Science and Health
Microbiology

December, 2016

MORPHOLOGICAL RESPONSES OF EUKARYOTIC CELLS TO SK-03-92

By Timothy J Green

We recommend acceptance of this thesis in partial fulfillment of the candidate's requirements for the degree of Master of Science in Biology: Microbiology Concentration.

The candidate has completed the oral defense of the thesis.

Anne Galbraith, Ph.D.
Thesis Committee Chairperson — 2/9/17 Date

Marc Rott, Ph.D.
Thesis Committee Member — 2/9/17 Date

Peter Wilker, Ph.D.
Thesis Committee Member — 2/9/17 Date

Mike Abler, Ph.D.
Thesis Committee Member — 2/9/17 Date

Thesis accepted

Steven Simpson, Ph.D.
Graduate Studies Director — 2/22/17 Date

ABSTRACT

Green, T.J. Morphological responses to SK-03-92 in eukaryotic cells. MS in Biology: Microbiology Concentration, December 2016, 70pp. (A. Galbraith)

SK-03-92, a modified form of a stilbene produced by *Comptonia peregrina*, has been shown to effectively kill a variety of gram-positive bacteria, but is not toxic in a mouse model. In this work, several morphological responses of wild-type *Saccharomyces cerevisiae* (yeast) to SK-03-92 treatment were observed by light microscopy. Although none of these morphological changes correlated with cell death, the responses did follow a general sequence. Previous studies of yeast mutants suggested that the mitochondria were a target of SK-03-92. Mitochondrial staining of wild-type and mutant yeast did reveal a statistically significant correlation between the proportion of cells killed by SK-03-92 and the percentage of cells containing mitochondrial abnormalities, confirming that mitochondria are a primary target of SK-03-92 in yeast. A human monocytic cancer cell line, THP-1, was also treated with a range of SK-03-92 concentrations, again revealing a statistically significant correlation between mitochondrial abnormalities and cell death, with punctate mitochondria observed with apoptotic death at low concentrations of SK-03-92, and diffuse mitochondria observed with necrotic death at high concentrations of SK-03-92. Together, these results indicate that mitochondria are likely the target of SK-03-92 in eukaryotic cells.

ACKNOWLEDGEMENTS

I would like to thank my major advisor, Dr. Anne Galbraith, for her guidance and support. I could not have asked for a better major advisor; you have been immensely helpful not only with my thesis project. Your warm personality made pursuing my master's degree an enjoyable experience. A big thanks to Dr. Marc Rott. Your guidance has been immensely helpful to me in many facets of my life. I learned to always approach ideas from multiple directions, and that you shouldn't be content after the first possible answer that comes to mind. Thank you, Dr. Peter Wilker, for being a part of my committee; your assistance was much appreciated. I learned from your calm demeanor that things happen out of our control, but are not worth getting frustrated about. I would like to thank Dr. Michael Abler for being a member of my thesis committee. I did not need to reach out for your assistance often, but you were always willing to help when I did. A special thanks to the late Dr. David Howard for teaching me so much about microscopy. The knowledge you passed on to me made my thesis research immensely easier and why I am proficient in so many microscopy techniques.

Most of all, I thank my family and friends for the endless support you have shown me throughout my life. Mom, without you I would be nowhere near the person I am today. Lucas, I always strive to set the best possible example for you as an older brother and am so glad that you are becoming so intelligent and hard working. Dad, our relationship has been stressful to say the least, but it has contributed to my determination in my life's pursuits.

This work would not have been possible without financial support from the UW-L Graduate Research, Service, Education and Leadership grant.

TABLE OF CONTENTS

PAGE

LIST OF FIGURES

FIGURE PAGE

INTRODUCTION

Antibiotic Resistance

Infectious diseases were the leading cause of death worldwide prior to the introduction of antibiotics in the 1930s and 1940s with sulfa drugs and penicillin, respectively. The discovery of antibiotics led to a dramatic drop in mortality, and the subsequent discoveries of streptomycin, chloramphenicol, tetracycline, erythromycin, and rifamycin, all prior to 1960, launched the antibiotic era (1). Antibiotics are classified as either bacteriostatic that prevent bacterial cell growth, or bactericidal that kill bacteria. Whether bacteriostatic or bactericidal, antibiotics are typically effective in aiding in the removal of infectious bacteria from the body. Even with the hundreds of antibiotics available presently, most them use one of only four basic methods of action: 1) interference with cell wall biosynthesis, 2) interference with protein biosynthesis, 3) interference with RNA and DNA biosynthesis, or 4) interference with folate biosynthesis (1). Currently, antibiotics are losing their effectiveness in treating infectious diseases because bacteria are becoming resistant. Bacterial resistance is due to either mutations in the bacteria or acquisition of genes by gene transfer (2).

A mutation resulting in antibiotic resistance is a random event where a gene has been altered in the bacterial cell to grant the cell the ability to survive in the presence of the antibiotic (3). The other process of acquiring resistant mechanisms is through gene transfer. This occurs when a bacterium either obtains resistance genes from the

environment (transformation), is infected by a bacteriophage containing donor bacterial DNA (transduction), or conjugates with another cell and genetic material is directly transferred through physical contact with the donor cell. Conjugation most commonly involves closely related bacteria, but transfer can also take place between distantly related bacteria (2). The selective pressure caused by antibiotics increases the frequency of resistance in a population (4).

Bacterial species have acquired several mechanisms that are responsible for their resistance to previously effective antibiotics. For example, an efflux system grants bacteria the ability to immediately flush a multitude of antibiotics from the bacterial cell before the antibiotic can affect the bacterium. Another mechanism is the ability to change the permeability of the bacterial cell by altering the composition of the outer membrane. Composition changes of the outer membrane can prevent antibiotics from entering the cell. Bacteria are also capable of inactivating antibiotics by modification of the structure of the antibiotic to a non-toxic form. An analogous mechanism is the altering of the molecular structure of the antibiotic target, thus preventing interaction between the antibiotic and the target (5).

Antibiotic resistance has been increasing in frequency since the 1950s and has been gaining international attention in recent years, with multiple antibiotic resistant bacterial strains rendering standard treatments ineffective. In 2013 antibiotic resistance was estimated to have led to $20 billion a year in additional direct medical costs and $35 billion a year in lost productivity in the U.S. (6). The first case of penicillin resistance in *Staphylococcus aureus* occurred in 1967, and by 1998, penicillin resistance had exploded to 34% of all cases of *Staphylococcus aureus* infections (7). This trend is observed with

almost all antibiotics, and is leading to increased hospitalizations, mortality rates, and treatment costs (5, 6). An example would be nosocomial enterococcal bacteremia, a hospital acquired *Enterococcus* blood infection. Standard treatment is typically ampicillin. However, many nosocomial strains now have a high level of resistance to ampicillin, leading to vancomycin being the standard treatment option. Some *Enterococcus* strains have even become vancomycin resistant *Enterococci* (VRE). The VRE infections have proven to be more lethal and more likely to reoccur than susceptible *Enterococci* (5, 8). Another example of resistant bacteria is *Staphylococcus aureus,* a primary cause of lower respiratory tract and surgical site infections. *Staphylococcus aureus* is the second leading cause of nosocomial bacteremia, and cardiovascular infections (9). Hospitalizations due to *S. aureus* infections have increased by more than 62%, with the number of methicillin resistant *S. aureus* (MRSA) cases more than doubling from 1999 to 2005 (9). Vancomycin is currently the drug of choice for MRSA infections. Unfortunately, vancomycin resistant strains are already beginning to emerge (9).

The acquisitions of these mechanisms of resistance have occurred quickly due to over-prescription of antibiotics that put bacteria under a selective pressure more frequently than necessary. Staying ahead of the wave of antibiotic resistant bacteria has proven difficult as development of novel antibiotics that work by new mechanisms has been slow (10). Many newly developed antibiotics are derivatives of previous antibiotics with alterations in their chemical structures. Because these drugs function similarly to their parent molecules, they are generally ineffective against bacterial strains that already show antibiotic resistance to the parent molecule (10).

When searching for novel antimicrobial compounds, natural sources have been historically successful (11). The antibiotic era began with the development of penicillin from a fungus, along with streptomycin, chloramphenicol, and tetracycline from soil bacteria. Chemists have attempted to synthesize antibiotic compounds *de novo*, but *de novo* synthesis has not been an effective approach because the long linear pathways required to synthesize compounds leads to low yields. For example, with step yields at 90%, a conservative ten-step pathway would result in a 35% yield at best (12). A successful approach has been to develop antibiotics by using the scaffold of naturally occurring antimicrobial compounds. From 1981 to 2003, 75% of new drugs treating infectious diseases came from natural sources (13).

A potential biological structure that could serve as an antimicrobial scaffold, the stilbene, was initially discovered in the 1890s, but not analyzed for antimicrobial activity until the 1980s (14). Stilbenes are produced by a variety of plant species for defensive purposes, and are composed of two aromatic rings linked by an ethylene bridge (FIG. 1A). This stilbene scaffold can have different moieties added to it by enzymatic activity in the plant giving the resulting compound different functionalities. A well-studied stilbene, resveratrol (FIG. 1B), is found in red wine, peanuts, and an array of plants. Resveratrol has shown anti-aging, anti-inflammatory, antioxidant, and anticancer activities in animal and human tissues (15). Resveratrol has also been shown to have both antibacterial and antifungal properties, among others (16). The membrane of bacterial cells and mitochondria of eukaryotic cells lose membrane potential when treated with resveratrol. The loss of membrane potential leads to an increase in reactive oxygen

species, which cause cellular damage (15). Bacteria and eukaryotic cells have also been observed to respond to resveratrol treatment with morphological changes, induction of apoptosis, changes in DNA content of cells, and interference with the cell cycle (17). Despite much research for well over a decade, the mechanism of action for resveratrol is still not understood.

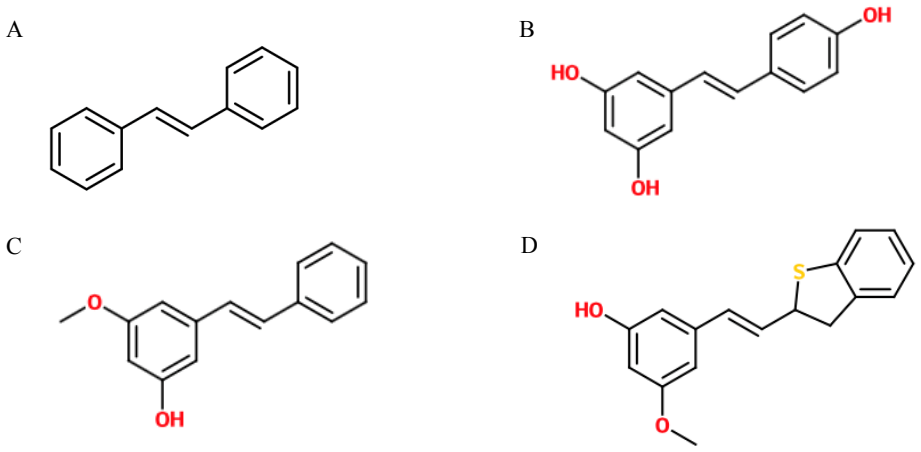

FIG. 1. Chemical structure of stilbenes. A generic representation of (A) a stilbene, (B) resveratrol, (C) stilbene extracted from *Comptonia peregrina*, and (D) the structural analog of the *C. peregrina* stilbene, SK-03-92.

Comptonia peregrina, commonly known as the sweet fern, produces stilbenes that have been used medicinally by the Native Americans of the great lakes and maritime regions for many years prior to contact with Europeans (18). The sweet fern has been used to treat a variety of ailments. The leaves are used for tea to alleviate diarrhea, headache, fever, inflammation of the mucous membranes, vomiting of blood, and rheumatism. The leaves also been applied directly to the skin to resolve skin infections, rash from poison ivy, pain from stings, and minor hemorrhages. Non-medicinal applications of the sweet fern included incense, preservation of fruit, and insect repellent. A molecular extract of the sweet fern was found to contain the active ingredient (E)-3-

hydroxy-5-methoxystilbene (FIG. 1C). (E)-3-hydroxy-5-methoxystilbene was purifiedfrom the leaves of the sweet fern and antimicrobial effects were observed when applied to several pathogenic bacteria species (18). A structural analog of (E)-3-hydroxy-5-methoxystilbene was developed by researchers at University of Wisconsin – Milwaukee, (E)-3-(2-(benzo[b]thiophen-2-yl) vinyl)-5-methoxyphenol, and given the code name SK-03-92 (19) (FIG. 1D). Using standard minimum inhibitory concentration (MIC) assays, SK-03-92 showed antimicrobial effects against a variety of gram-positive bacteria including important disease causing agents such as MRSA and VRE strains, *Clostridium, Enterococcus*, *Corynebacterium*, *Mycobacterium*, *Peptostreptococcus*, and *Streptococcus* species (19). The antimicrobial effects of SK-03-92 were shown to be more potent than the normal sweet fern stilbene, with MICs against gram-positive bacteria for SK-03-92 being four to 16-fold lower than MICs for (E)-3-hydroxy-5-methoxystilbene (18, 19).

SK-03-92 was tested for its ability to treat an active infection by using mice models that were infected with *S. aureus* in a hind limb. SK-03-92 was injected into the peritoneal cavity of the infected mice. A hormetic response to SK-03-92 was seen, with high and low concentrations failing to clear infection, and medial concentrations resulting in a two-log reduction in *S. aureus* cells with no observable negative effects to the mouse model (20). The lack of negative effects of SK-03-92 in the mouse model suggested that SK-03-92 may not affect human cells. However, further pursuits showed that SK-03-92 was lethal to single-celled fungi, *S. cerevisiae*, and a human cancer cell line, THP-1 cells (see below).

Types of Cell Death

Cell death in eukaryotes can occur in several ways. The different types of death form a spectrum that share characteristics with one another (21). Necrosis is at one end of that spectrum, a non-physiological death that occurs from external factors such as infections, toxins, or physical traumas, that does not require energy (22). Apoptosis is at the other end of the spectrum, and is a programed cell death that requires energy (21, 23). Between necrosis and apoptosis, cell death prosses share properties of both, such as necroptosis (24). Only necrosis and apoptosis will be considered below.

Necrosis

In metazoans, necrosis almost always has negative impacts. Necrosis involves the unregulated digestion of cellular components by enzymes released from lysosomes. The release of the digestive enzymes causes significant cell damage. The cell damage results in swelling of many cellular components, including the mitochondria. Swelling is followed by an uncontrolled lysis of the cell, releasing cell debris into extracellular spaces. The cell debris from necrotic cells initiates an inflammatory response, which can prevent phagocytosis of necrotic cells and lead to further damage (22). Removal of necrotic cells is a slow process due to the disorganized death and large amounts of cell debris (25).

Apoptosis

Unlike necrosis, apoptosis is an organized death pathway and serves a vital process in metazoans in cell turnover, development, and aging, as well as responses to early infection, damage, and cancer (26). Apoptotic death involves unique and specific morphological and biochemical changes. Nuclear shrinkage and disassembly of the cell

into apoptotic bodies is a generalized example of an apoptotic morphological change. This fragmentation of the apoptotic cell leads to phagocytosis of individual cells by macrophages and adjacent cells without associated inflammation. The removal of apoptotic cellular material occurs faster than removal of necrotic material (23). Apoptosis also includes biochemical changes, such as nuclear DNA fragmentation and caspase activation (21, 23). Damaged mitochondria can play a major role in initiating the apoptotic response through the release of Bcl-2 proteins that activate the caspase cascade (27).

Programmed Cell Death in Unicellular Organisms

Unicellular eukaryotes and bacterial communities benefit from individual cells undergoing an apoptotic-like cell death as well. Referred to only as programmed cell death in unicellular organisms, this process appears to be like apoptosis in metazoans. Although cell death is not beneficial for an individual cell, death of a single cell can benefit a population of cells, "behaving" like a multicellular organism (28). For example, the removal of cells via programmed cell death can limit viral transmission by resulting in a less dense population, add nutrients to the environment from cells that undergo programmed cell death, reduce nutrient consumption, and/or decrease mutation rate in the population due to fewer cells. To prevent decimation of an entire population of cells, many bacteria have a small percentage of cells, persisters, which do not undergo programmed cell death because they have other survival mechanisms (28).

Persisters

Persisters are a subpopulation (approximately 1 to 10%) of an otherwise antibiotic susceptible population of unicellular organisms that survive antibiotic treatment. The

persisters are not antibiotic resistant in the classic sense. When regrown the persisters become susceptible to the antibiotic once again, with only a 1 to 10% subpopulation surviving antibiotic treatment. In a population, normal cells become persisters through phenotype switching to maintain a constant 1 to 10% subpopulation of cells that can survive in the presence of selective pressure by an antibiotic (28). The persister phenomenon appears to be an epigenetic phenotypic variation in bacterial cell populations and leads to concerns when treating chronic bacterial infections in humans (29, 30).

Biofilms play an important role in recurring infections by producing a barrier between the host immune system and the bacterial cells. When an antibiotic treatment is introduced, normal bacterial cells exposed to the antibiotic are killed. Planktonic persisters are removed via the immune system, but the persisters in the biofilm are protected from the host immune system. After antibiotic concentrations are reduced, persisters begin to repopulate the biofilm (31). A population of cells appear to always retain a subpopulation of persisters with a lower percentage of persisters in lag and early exponential stages of growth, and a higher percentage of persister cells in mid-exponential to stationary phase (32). The persister phenotype is unstable and the persister cells are slower growing with high changeover rates to normal non-persister cells (31). The stability of these persisters increases when an antibiotic is present due to selective pressure on the population. Once the antibiotic is removed the survivability tips back to favor normal cells due to the higher metabolic activity and increased cell division of normal cells. This leads to a decrease in the persister population back down to the typical 1 to 10% of the bacterial population via phenotype switching (32). The persister

phenotype is believed to provide a bet hedging strategy that benefits a population of bacterial cells by acting as a preventative measure to ensure survival of the population in the presence of an otherwise lethal event (33).

Saccharomyces cerevisiae

Saccharomyces cerevisiae is a unicellular budding yeast commonly known as baker's or brewer's yeast because it is used to make bread and beer products. *S. cerevisiae*, which will be referred to as yeast in this thesis, serves as a valuable experimental model for many reasons. Yeast has strongly conserved basic functions and pathways that are found in higher multicellular organisms. Yet is also relatively inexpensive to work with and requires little to no precautionary measures as yeast cells are not pathogenic. Yeast cells are relatively large in comparison to other single celled organisms such as bacteria, making them easier to observe when using microscopy imaging. Arguably the greatest advantage of working with yeast cells, however, is their well-annotated genome and variety of genetic tools and deletion strains. The genome is completely sequenced, well understood, and almost completely free of introns making cloning of genes and modifications relatively easy (34). Various groups have worked to develop a panel of strains with mutations in all non-essential genes (35) allowing function of gene products and phenotypes of mutant strains to be readily observed (36).

THP-1 Cell line

A former graduate student at UWL observed that THP-1 monocytes that were differentiated into macrophages by treatment with phorbol 12-myristate 13 acetate were killed by SK-03-92, also resulting in "persisters" (37). The THP-1 cell line was originally isolated from a young male suffering from acute monocytic leukemia. The THP-1 cancer

cell line shares numerous characteristics with normal monocytes including morphology, secretion products, membrane antigens, and expression of genes involved with lipid metabolism (38). These cells are also larger than bacteria and yeast cells making for easier observations and imaging via microscopy.

Preliminary Data

The Galbraith lab has shown that yeast cells are killed by SK-03-92 at concentrations of 4 μg/mL and higher by both MIC and a simple plating assay (unpublished observations). Like bacteria, yeast cell populations do not die completely when treated with SK-03-92, retaining about 1 to 10% "persisters". These persisters are of two types: those that grow at a slower rate, and those that grow into normal-sized colonies. The small yeast colonies are, called petites, a phenomenon due to yeast cells that cannot respire and therefore grow more slowly, as they use fermentation to generate ATP (39). The resistance of petite cells with defective mitochondria led our lab to hypothesize that active mitochondrial function is necessary for SK-03-92 to be lethal to yeast. The Galbraith lab has also shown that yeast cells in stationary phase or growing anaerobically, two conditions that decrease or eliminate the need for mitochondrial function, are not appreciably killed by SK-03-92 treatment (unpublished observations). Preliminary observations have also shown that the normal mitochondrial network of wild-type yeast is dramatically affected by treatment with SK-03-92.

In addition to yeast cells dying in response to SK-03-92, the Galbraith lab has observed several interesting morphological responses. The morphological responses include enlargement of vacuoles with contents, phase bright inclusions, abnormal cell wall, and pitting. Similar changes were observed in bacteria and THP-1 cells (data not

shown) (37). Regardless of the time and/or concentration of SK-03-92, however 1% of the cells persisted, but when allowed to grow in the absence of SK-03-92 for 24 hours, the persisters grew into a population that was once again susceptible to SK-03-92, with approximately 1% surviving. Together, these data suggested that cells needed to be aerobically growing and/or metabolically active for SK-03-92 to be lethal, albeit with 1% persisters. With that hypothesis in mind, we began testing a variety of mutants defective in processes related to mitochondria or mitochondrial function as the mitochondria may be involved in the mechanism of action for SK-03-92. Other stilbenes, such as resveratrol, have also been observed to affect the mitochondria (15).

The lethal effect of SK-03-92 on yeast gave value to the investigation of various yeast mutants. The sensitivity or resistance of mutants relative to wild-type yeast helped determine which mutants to examine microscopically in this work. The sets of mutants where chosen for microscopic examination after treatment with SK-03-92, those involved in mitophagy, the glyoxylate cycle, and mitochondrial DNA repair. The mitophagy yeast mutants, *atg11* and *atg32*, were selected for further investigation because of their approximate 10 to 100-fold greater sensitivity to SK-03-92 treatment than wild-type yeast (FIG. 2A, 2B). The *ATG11* and *ATG32* genes are specific to mitophagy, and are needed for the initiation of the mitophagy process. Mitophagy is a form of autophagy where defective or unneeded mitochondria are selectively degraded (40). The sensitivity of these mitophagy mutants suggested that mitochondria are a target of SK-03-92. The ability to rid a eukaryotic cell of defective mitochondria is vital to cell health. Damaged or stressed mitochondria are typically selected for mitophagy to prevent further cell damage (40). Healthy mitochondria can also be selected for degradation, although this

usually occurs under starvation conditions, when the cell does not need as many mitochondria (40). The Atg32 protein, a major component of mitophagy in yeast, localizes to selected mitochondria to initiate the mitophagy process by recruiting a second protein, Atg11 (FIG. 3) (40, 41). The selected mitochondria are eventually moved to the vacuole where degradation of the mitochondria occurs (mitophagy) (42), or the vacuole is moved to the cell membrane and the contents of the vacuole are released from the cell (mitoptosis) (42, 43, 44).

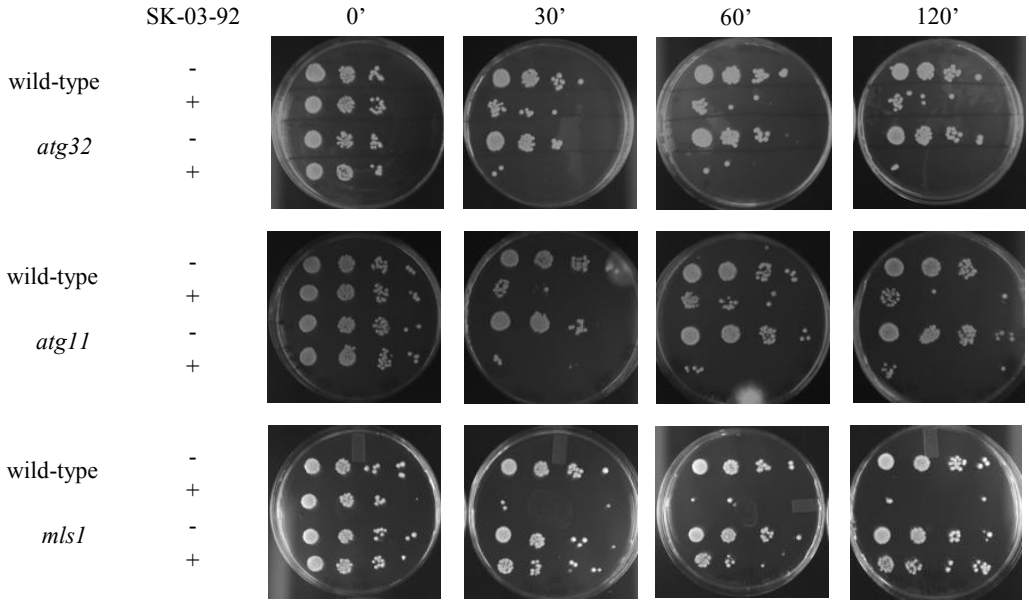

FIG. 2. Spot assays of wild-type and yeast mutants. Wild-type, *atg32*, *atg11*, or *mls1* mutants were treated with 8 µg/mL SK-03-92 (+) or an equal volume of DMSO (-) and samples diluted and plated after 0’, 30’, 60’, and 120’ as described (Materials and Methods).

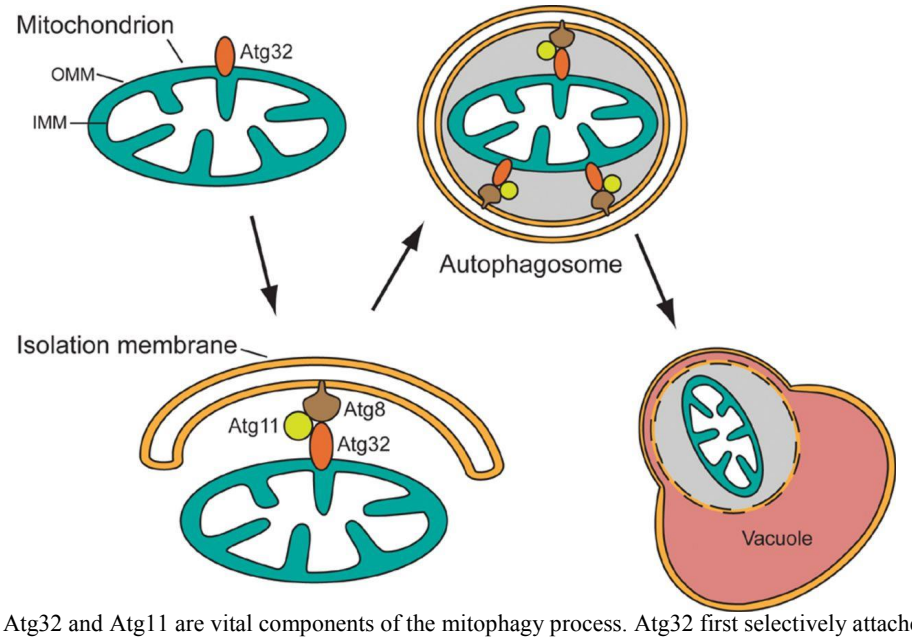

FIG. 3. Atg32 and Atg11 are vital components of the mitophagy process. Atg32 first selectively attaches to mitochondria. Atg11 then attaches to Atg32 and aids in attachment to an isolation membrane. This attachment to the isolation membrane leads to the mitochondria being escorted into an autophagosome and eventually moving into the vacuole (41).

A group of yeast mutants directly involved with the glyoxylate pathway (*cit2*, *icl1, mls1*) was also selected for further investigation microscopically. The glyoxylate yeast mutants were 10 to 100-fold more resistant to SK-03-92 treatment than wild-type yeast (see FIG. 2C for data from *mls1* mutant). The glyoxylate pathway is a variation of the tricarboxylic acid (TCA) cycle that allows cells to use 2-carbon compounds to restore NAD+/NADP+ levels to produce energy and perform essential anabolic reactions. Although the TCA and glyoxylate cycle are similar in many ways there are significant differences. The glyoxylate cycle pathway occurs in peroxisomes (45), and the TCA cycle occurs in the matrix of the mitochondrion in eukaryotic cells (46). Both the glyoxylate cycle and TCA cycle occur along the inner surface of the cell membrane in the cytoplasm of bacteria (47). The full TCA cycle is found in most organisms and portions of the TCA cycle are found in almost all organisms. The TCA cycle is a key pathway

that connects the metabolism of carbohydrates, proteins, and fats together. The full TCA cycle is catabolic in nature and consists of eight enzymes that function to oxidize acetate (acetyl-CoA) to two water and two carbon dioxide molecules. The reactants used in a single pass through the TCA cycle are three NAD^+, one FAD, and one GDP, which result in the production of three NADH + H^+, one $FADH_2$, and one GTP, as the products respectively (45). The NADH + H^+ and $FADH_2$ are used in oxidative phosphorylation reactions to produce ATP (46).

As opposed to the TCA cycle the glyoxylate cycle is not found in all organisms. The glyoxylate cycle is typically found only in plants, bacteria, protists and fungi. The location of the glyoxylate cycle reactions can vary depending on the organism, but is generally observed in peroxisomes of eukaryotes (FIG. 4) (45). The glyoxylate cycle occurs along the inner cell membrane of bacteria in the cytoplasm (47). The glyoxylate cycle shares five of the eight enzymes of the TCA cycle (FIG. 5) (45). The glyoxylate cycle is also known as the glyoxylate bypass as isocitrate is converted to succinate and glyoxylate, bypassing the decarboxylation steps of the TCA cycle. Unlike the catabolic TCA cycle, the glyoxylate cycle is anabolic due to the bypass of the decarboxylation steps. Bypassing the decarboxylation steps conserves two carbon atoms for biosynthesis (45). The succinate can be transferred out of the peroxisome and used for other cellular processes, such as biosynthesis or the TCA cycle. The glyoxylate molecule produced is combined with acetyl-CoA to form malate. Malate either continues in the glyoxylate cycle, is transported to the mitochondria, or is used for biosynthesis. The glyoxylate cycle converts two acetyl-CoA and NAD+ molecules to succinate and NADH+, respectively, and allows growth of yeast cells on acetate. The final mutant selected for microscopic

investigation was *ogg1*. The *ogg1* mutant was approximately 100 times more resistant to SK-03-92 treatment than wild-type. The Ogg1 protein repairs oxidative damage to mitochondrial DNA and contributes to ultraviolet radiation resistance (48).

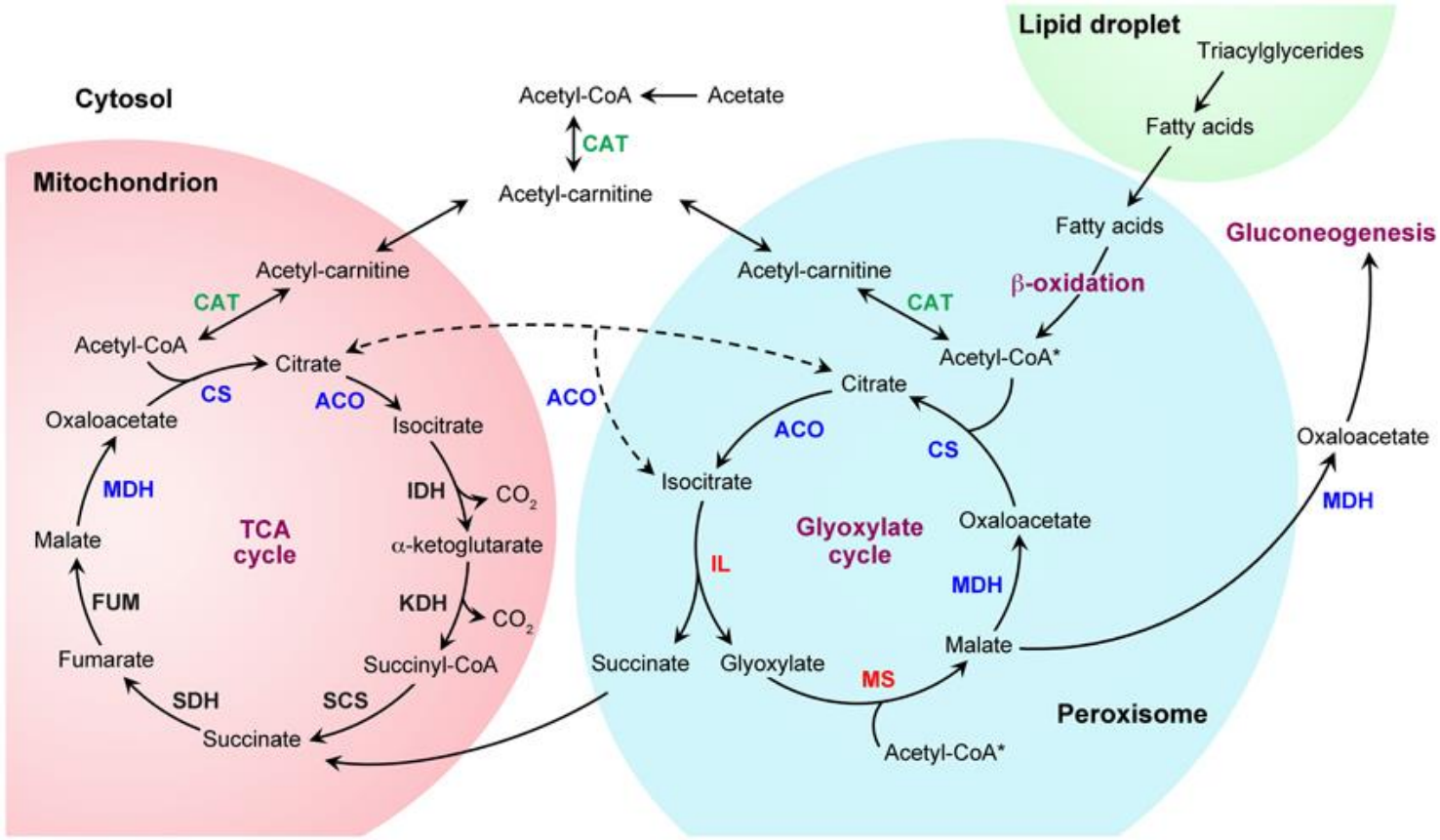

FIG. 4. The glyoxylate cycle occurs in the peroxisome of most eukaryotic cells while the tricarboxylic acid cycle always takes place in the matrix of the mitochondrion (45).

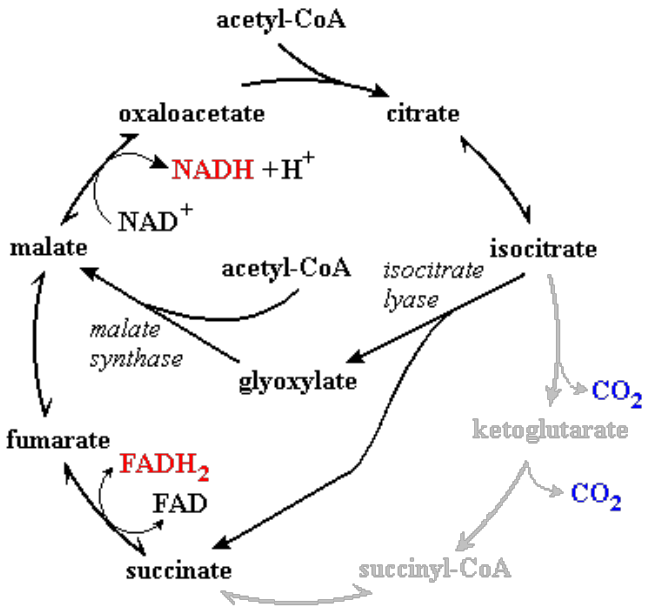

FIG. 5. An overlay of the glyoxylate and TCA cycles. The reactions involved with the TCA cycle are those that form the outer ring (including the gray reactions). The reactions involved with the glyoxylate cycle are all reactions that are not shaded gray (45).

Research Objectives

SK-03-92 has antimicrobial properties against several pathogenic bacteria that include *B. cereus*, *L. monocytogenes*, *E. faecium*, *S. aureus*, and antibiotic resistant bacterial strains (19). The antimicrobial properties of SK-03-92 make it a compound worth pursuing clinically. SK-03-92 could help in the fight against the increasing prevalence of antibiotic resistant microbes. However, before a company would consider licensing SK-03-92 as an antimicrobial, a mechanism of action must be determined. Yeast provides a good genetic system to use in this process, and the size of THP-1 cells are optimal for imaging microscopically to observe cell responses to SK-03-92.

The research in this thesis was done to continue the investigation of how SK-03-92 works by observing, via various microcopy techniques, the morphological responses

of yeast and THP-1 cells. The observed responses to SK-03-92 were quantified and analyzed to see if specific responses correlated with cell death. Yeast mutants were used to see if responses to SK-03-92 differed from wild-type yeast based on their sensitive or resistant phenotypes by plating assays. Additionally, yeast cells were arrested in, or synchronized and released from, G1, G1/S, or G2/M phase to determine if SK-03-92 shows greater lethality at a specific point in the cell cycle. Other compounds have been shown to be more effective at killing eukaryotic cells when they are in a specific stage of the cell cycle. For example, etoposide, a compound that binds to and inactivates topoisomerases, kills cells in S phase better than cells in other phases (49). If lethality of SK-03-92 does differ at cell cycle points it may contribute to understanding the mechanism of action.

MATERIALS AND METHODS

Strains and Media for Yeast

Standard media and techniques used to work with *Saccharomyces cerevisiae* were as described (50). Yeast strains are listed in Table 1.

TABLE 1. Yeast Strains used in this study.

Strain Name	Genotype	Affected Pathway
BY4741 [1]	***a**, his3, leu2, met15, ura3*	N/A
BY4742	*α, his3, leu2, met15, ura3*	N/A
BY4742- *atg11*	*α, his3, leu2, met15, ura3,* YPR049c::*kanmx4*	Mitophagy
BY4742-*atg32*	*α, his3, leu2, met15, ura3,* YIL146c:: *kanmx4*	Mitophagy
BY4742-*cit2*	*α, his3, leu2, met15, ura3,* YCR005c:: *kanmx4*	Glyoxylate Cycle
BY4742-*mls1*	*α, his3, leu2, met15, ura3,* YNL117w:: *kanmx4*	Glyoxylate Cycle
BY4742-*icl1*	*α, his3, leu2, met15, ura3,* YER065c:: *kanmx4*	Glyoxylate Cycle
BY4742-*ogg1*	*α, his3, leu2, met15, ura3,* YML060w:: *kanmx4*	Mitochondrial DNA Repair

[1] All strains are from EuroSCARF (51).

Treatment of Yeast with SK-03-92

Wild-type (BY4742) or mutant yeast (Table 1) were inoculated, using a single colony from YPD plates, into 5 mL yeast extract-peptone-acetate (YPA) medium as described (50) and grown overnight in a 50 mL Erlenmeyer flask, shaking at 200 rpm at

30°C. Cell concentration of the overnight culture was determined using a hemocytometer. Cells were diluted into 11 mL fresh YPA medium at a concentration of $2X10^6$ cells/mL and incubated at 200 rpm at 30° C for two hours. The culture was then subdivided into two 5 mL cultures and either treated with a final concentration of 8 μg/mL SK-03-92 in DMSO, or an equal volume of DMSO as a negative control.

Quantification of Yeast Morphology Responses

Wild-type (BY4742) yeast cells were treated with SK-03-92 as described above. Samples of 900 μL were taken immediately before treatment (0), and 0.5, 1, 2, 4, 6, 8, 10, 12 and 24 hours after treatment and added to 100 μL of 37% formaldehyde for storage at room temperature. Samples were visualized and morphological states were observed and quantified using various forms of microscopy (see "Microscopy" for specifics). At least 500 cells were counted at each timepoint. A multinomial logistic regression was used to compare the number of normal cells versus the number of cells with each abnormal morphology.

Quantification of Yeast Mitochondria Morphology Responses

Wild-type (BY4742) or mutant yeast strains were treated with SK-03-92 as described above. Thirty minutes prior to treatment (1.5 hours after dilution) MitoTracker Red CMXRos (Thermo Fisher Scientific, Waltham, Massachusetts) was added to a final concentration of 100 nM. Samples were taken immediately before treatment (0) and 1, 5, 10 and 15 minutes after treatment. Samples were immediately visualized and quantified via microscopy under live conditions (see "Microscopy" for specifics). At least 100 cells were counted at each timepoint. A logistic regression was used to compare the number of cells with normal mitochondria versus the number of cells with abnormal mitochondria.

Quantification of Yeast Viability

Standard culture preparation and SK-03-92 treatment was performed for wild-type and all mutants, as described above. Thirty minutes prior to treatment (1.5 hours after dilution) 5 μL of Syto 9, and 5 μL of propidium iodide was added from the Live/Dead FungaLight Yeast Viability Kit (Molecular Probes, Eugene, Oregon). Samples were taken before treatment T (0) and 0.5, 1, 1.5, 2, 2.5, 3, 3.5, and 4 hours after treatment. Samples were immediately observed and quantified via microscopy (see "Microscopy" for specifics). At least 300 cells were counted at each timepoint. A logistic regression was used to compare the number of propidium iodide negative versus the number of propidium iodide positive cells.

Yeast Cell Cycle Arrest Assay

Wild-type strain BY4741 was grown up and diluted to $2X10^6$ cells/mL as described above. Immediately following dilution, the culture was either treated with either a final concentration of 5 μg/mL of alpha factor for G1 phase arrest, 0.2M hydroxyurea for S phase arrest, or 15 μg/mL nocodazole for G2/M phase arrest. A second treatment was added after 1.5 hours of incubation. Cultures were considered arrested when >95% of cells were at the appropriate arrest point as evidenced by light microscopy. Cells were subdivided into 5 mL cultures and treated with a final concentration of 8 μg/ml of SK-03-92 or an equal volume of DMSO. Samples were taken before treatment (T0) and 0.5, 1, 2, and 24 hours post treatment, and diluted to 10^{-1}, 10^{-2}, 10^{-3}, and 10^{-4}. Ten microliters of each dilution were spotted onto YPD plates and allowed to incubate for 2-3 days at 30°C before analysis.

Yeast Cell Cycle Synchronization Assay

A second variation of the experiment above followed the same protocol except that cells were released from arrest prior to SK-03-92 treatment by washing cells twice with fresh YPA. Cells were divided into 5 mL cultures and treated with a final concentration of 8 μg/ml of SK-03-92 or an equal volume of DMSO. Samples were taken before treatment (T0) and 0.5, 1, 2, and 24 hours post treatment, and diluted to 10^{-1}, 10^{-2}, 10^{-3}, and 10^{-4}. Ten microliters of each dilution were spotted onto YPD plates and allowed to incubate for 2-3 days at 30°C before analysis.

Treatment of THP-1 Cells

Standard media and techniques were used for THP-1 cells as described (52). Approximately $2x10^5$ cells were centrifuged at 150 Xg for 5 minutes. Cells were suspended in 2 mL of pre-warmed RPMI1640 Strep Pen (Thermo Fisher, Waltham, Massachusetts) resulting in a final cell concentration of $1X10^5$ cells/mL. THP-1 cells were then treated with a final concentration of 5 μg/mL, 10 μg/mL, 15 μg/mL, 20 μg/mL, or 25 μg/mL of SK-03-92, or an equal volume of DMSO, vortexed, and transferred to a glass bottom dish (MatTek, Ashland, Massachusetts).

Quantification of THP-1 Mitochondria Responses

THP-1 cells were set up for SK-03-92 treatment as described above. After dilution of cells into 2 mL of media, MitoTracker Red CMXRos (Thermo Fisher, Waltham, Massachusetts) was added to a final concentration of 100 nM. Cells were incubated for 30 minutes before SK-03-92 treatment and transfer. Mitochondrial morphologies were visualized under live conditions via microscopy (see "Microscopy" for specifics). A multinomial logistic regression was used to compare the number of

THP-1 cells with normal mitochondria versus the number of THP-1 cells with abnormal mitochondria.

Annexin V Analysis of THP-1 Cells

THP-1 cells were set up for SK-03-92 treatment as described above. After dilution of cells into 2 mL of media, 5 µL of FITC Annexin V and 5 µL of Propidium Iodide were added from the FITC Annexin V Apoptosis Detection Kit (BD Biosciences, San Diego, California) and THP-1 cells were incubated for 30 minutes before SK-03-92 treatment and transfer. Viability of the cells was determined under live conditions via microscopy (see "Microscopy" for specifics). A multinomial logistic regression was used to compare the number of cells negative for both FITC Annexin V and Propidium Iodide versus the number of cells positive for either FITC Annexin V, Propidium Iodide, or both.

Microscopy

Light microcopy: Phase Contrast/DIC

The Nikon 80i microscope with objective 100X/1.30 Oil N.A. 0.17 WD 0.16 (for DIC) and 100X/1.40 Oil N.A. 0.17 WD 0.13 (for phase contrast) was used for visualization and quantification of yeast morphologies when treated with SK-03-92.

Epifluorescence

An X-cite mercury lamp was used as an excitation source for all microscopes. Filter cubes were used for multiple fluorescence channels. Blue fluorescence was detected using a DAPI filter cube with excitation (EX) of 340-380 nm, dichromatic mirror (DM) of 400 nm and barrier (BA) of 435-485 nm. Green fluorescence was detected using a

GFP filter cube with EX of 480/40 nm, DM of 505, and BA of 535/50. Red fluorescence was detected using TRITC filter with EX of 540/25, DM of 565, BA of 605/55.

Imaging

An ExiAqua camera (QImaging) and NIS Elements imaging software was used with the Nikon 80i microscope to obtain all images. Images were enhanced using ImageJ software (53).

Inverted Microscope

The Nikon Eclipse TE2000-U was used for observation and quantification of live THP-1 cells in a glass bottom dish with 100X/1.40 Oil N.A. 0.17 WD 0.13.

RESULTS

Wild-Type Yeast Cells Show Morphological Responses to SK-03-92

Preliminary data in the Galbraith lab had indicated that morphological changes occurred in response to treatment of yeast with SK-03-92. Morphological categories chosen for analysis were those that were commonly observed in this study and included cells that were normal, or had enlarged vacuoles with contents, phase bright inclusions, abnormal cell walls, and/or pits (FIG. 6). Yeast cells were treated with SK-03-92 as described (Material and Methods) for up to 24 hours. Phase contrast and DIC microscopy were used to quantify the number and the timing of the yeast cells' responses. The normal untreated morphology included cells with a smooth appearance on the cell surface using DIC microscopy (FIG. 6A), and a solid, phase dark cell as observed using phase contrast microscopy (FIG. 6B). Enlarged vacuoles with contents were observed in cells by DIC as large pseudo-depression in the cell with one or more contents appearing as spheres within the depression (FIG. 6C). Using phase contrast, the yeast cells with enlarged vacuoles with contents had an enlarged vacuole, with one or more spherical contents that appeared as phase dark balls within the enlarged vacuole (FIG. 6D). These phase dark spheres have been described in literature as autophagic bodies (54) and are characterized by their rapid, apparently random, movement within the vacuole.

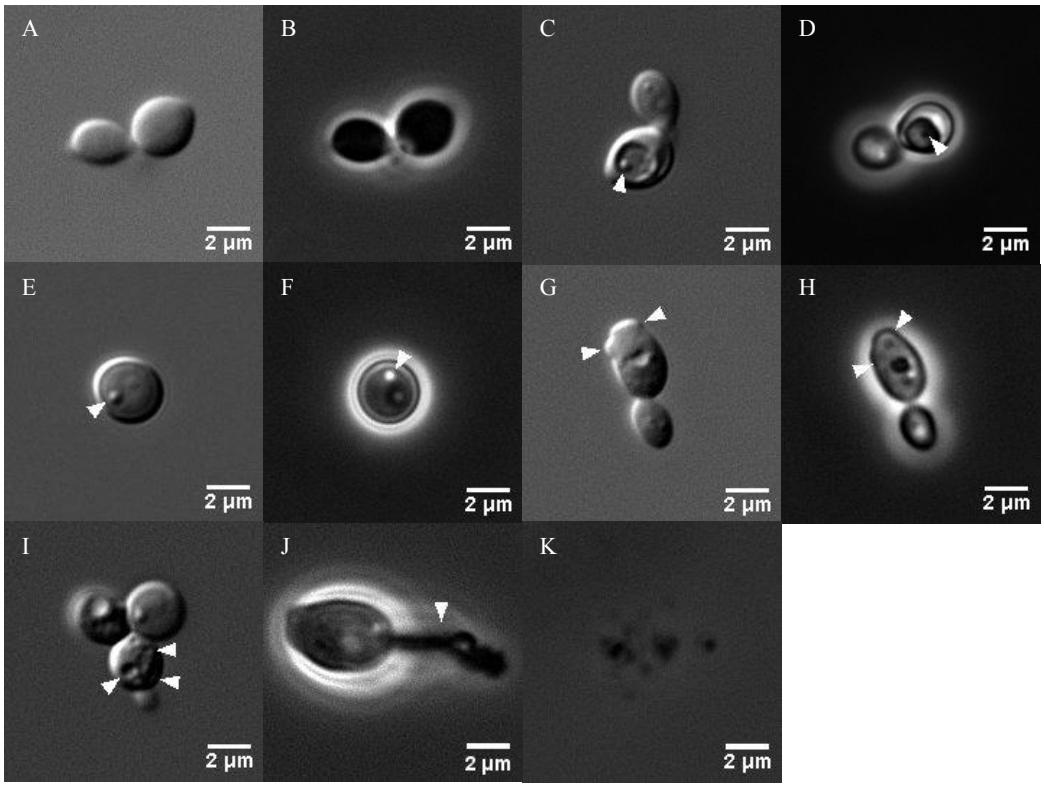

FIG. 6. Representative images of responses observed in wild-type yeast cells treated with 8 µg/mL SK-03-92. Wild-type yeast cells were treated and examined using DIC and/or phase contrast with a 100X oil immersion objective. (A) Normal wild-type yeast cells showed a smooth cellular surface with DIC and a (B) solid phase dark image with phase contrast. (C) Enlarged vacuoles appeared as depressions in the cells with the contents appearing as spherical bulges (arrow head). (D) With phase contrast, enlarged vacuoles appeared as phase light spherical regions within the yeast cells with a phase dark outline with contents appearing as phase dark balls (arrow head). (E) Phase bright inclusions under DIC appeared as spherical bulges (arrow head) not within a vacuole or (F) as phase bright spheres (arrow head) not within vacuoles using phase contrast. (G) Cells with abnormal cell walls displayed irregularities in the cell wall that appeared as non-spherical bulges (arrow heads) under DIC and (H) phase contrast. (I) Pits (arrow head). (J, K) Other responses that were not quantified but observed were beads on a string and extracellular debris fields.

Phase bright inclusions could be observed in cells using DIC as spherical bulges on the cell surface (FIG. 6E), but were observed using phase contrast where they appeared as phase bright spheres (FIG. 6F). Phase bright inclusions were similar to vacuole contents in size and shape, but were not found within the vacuole and did not move. Cells were defined as having abnormal cell wall if they had irregularities in the cell wall ranging from minor bulges to large blebs. The bulges and blebs of the abnormal

cell wall differed from the bulges caused by the phase bright inclusions as the cell wall abnormalities lacked a uniform spherical shape, and were easily observed under DIC (FIG. 6G). Using phase contrast, the cell wall abnormalities appeared as irregularities in the outline of the cells that were not phase bright (FIG. 6H).

The pitted cells could only be observed using DIC. The pits appeared as small depressions on the cell surface (FIG. 6I). Four yeast responses to SK-03-92 were observed but not enumerated due to the rarity of their appearance and not at every timepoint. One response called “beads on a string” (FIG. 6J) (55) was estimated to be observed in about 1/1000 yeast cells at the highest frequency. Cell rounding (FIG. 6E, 6F) was estimated to be observed in about 1/300 yeast cells at the highest frequency. Cell swelling was estimated to be observed in about 1/400 cells at its highest frequency. The extracellular debris fields (FIG. 6K) were seen frequently, but were not quantifiable because the number of cells contributing to a given debris field was not possible.

Changes in morphological responses by yeast cells treated with SK-03-92 over time were shown to be significant (p value= 0.0001) using a multinomial logistic regression to compare the number of normal cells versus the number of cells with each abnormal morphology. Five-hundred cells per timepoint were categorized based on the morphological responses described in FIG. 6. It was determined that the morphological changes in yeast cells treated with SK-03-92 followed a specific chronological sequence. The frequency of cells with a normal morphology decreased over time through 12 hours of treatment, rebounding slightly after 24 hours (FIG. 7). (Note that no timepoints were taken between 12 and 24 hours.) The frequency of cells containing enlarged vacuoles and autophagic bodies increased for the initial two hours after SK-03-92 treatment as the

frequency of normal cells declined. After two hours of SK-03-92 treatment, the frequency of cells with enlarged vacuoles and contents decreased as the frequency of cells containing phase bright inclusions increased. The frequency of cells with phase bright inclusions continued to increase until 12 hours of treatment and then declined. The frequency of cells with abnormal cell walls showed a similar increase to the frequency of cells with phase bright inclusions, albeit delayed, and increased from 12 and 24 hours, while the frequency of cells with phase bright inclusions was decreasing. The frequency of cells with a pitted morphology increased within the first hour and remained relatively constant throughout 24 hours of treatment (FIG. 7).

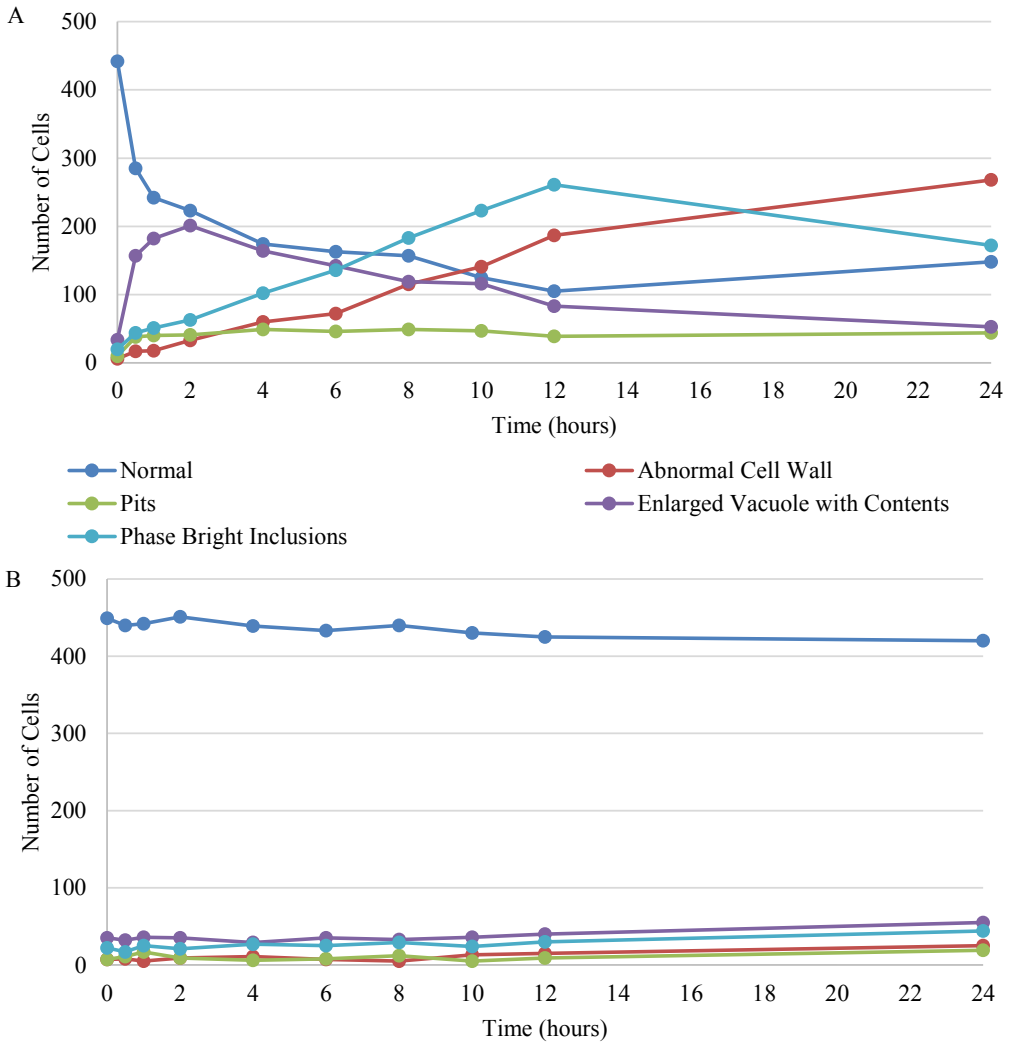

FIG. 7. Quantitative analysis of wild-type yeast cells treated with SK-03-92. (A) Cells treated with 8 µg/mL of SK-03-92 as described (Materials and Methods). (B) Cells were treated with DMSO to serve as a negative control. Samples at each timepoint were stored in 3.7% formaldehyde prior to examination. A total of 500 cells were observed by DIC and phase contrast microscopy. Each instance of an abnormality was counted in the total, including when one cell displayed multiple abnormalities.

SK-03-92 Causes Mitochondrial Abnormalities in Yeast

Wild-type and mutant yeast cells with normal mitochondrial networks display a tubular network that stretches throughout the cell (FIG. 8A) (56). Abnormal mitochondrial networks appeared in response to SK-03-92 treatment and were divided

into two morphological subgroups. Abnormal mitochondria were either punctate (FIG. 8B), or diffuse (FIG. 8C) where the whole cell was stained with MitoTracker Red. Most often, individual yeast cells treated with SK-03-92 showed both abnormal mitochondrial morphologies. Other abnormal characteristics observed included cells with a decrease in fluorescence intensity, fluorescently stained contents inside an enlarged vacuole (FIG. 8D, 6E), and extracellular fluorescently stained debris (FIG. 8F).

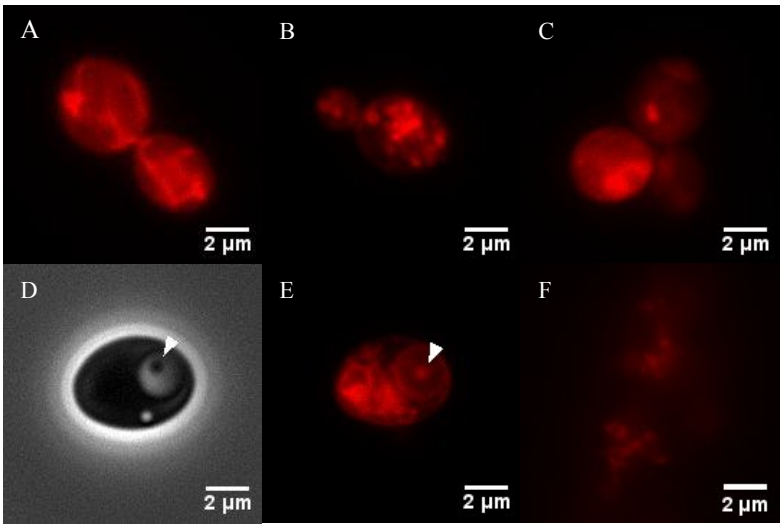

FIG. 8. Representative images of mitochondria of wild-type and mutant yeast treated with SK-03-92. (A) Normal mitochondrial networks were tubular and stretch throughout the yeast cell. Abnormal mitochondrial networks in response to SK-03-92 treatment displayed two characteristics that were almost always observed together in a single cell, (B) punctate and (C) diffuse. The contents of enlarged vacuoles did fluoresce red in some cells, indicating that the contents included mitochondrial components. (D) A phase contrast image of a cell with an enlarged vacuole with contents (arrow head) and (E) the same cell under fluorescence with the enlarged vacuole contents fluorescing red (arrow head) are shown. (F) Extracellular mitochondrial debris fields that stained red were also observed.

Mitochondrial responses induced by SK-03-92 treatment were evaluated among the panel of mutant strains and wild-type yeast (FIG. 9). Mutants chosen included mitophagy mutants that were more sensitive to lethality by SK-03-92, and glyoxylate cycle/mitochondrial DNA repair mutants that were more resistant to the lethal effects of SK-03-92 (unpublished observations, see also FIG. 2). As expected, wild-type and

mutant yeast strains differed in their percentages of normal mitochondria even when untreated (FIG. 9A). Wild-type had 100% normal mitochondria at time zero. Mitophagy mutants, *atg11* and *atg32*, had 82 % and 51% normal mitochondria at time zero, respectively. Glyoxylate mutants, *cit2*, *icl1*, and *mls1*, had 98%, 98%, and 99% normal mitochondria at time zero, respectively. The mitochondrial DNA repair mutant *ogg1* had 79% normal mitochondria at time zero. After 5, 10, and 15 minutes of treatment with SK-03-92 all wild-type and mutant strains yeast had less than 75%, 50%, and 30% of the yeast cells with normal mitochondrial networks, respectively. After 15 minutes of SK-03-92 treatment, wild-type, and the sensitive mitophagy mutants, *atg11* and *atg32*, had the lowest percentage of yeast cells with normal mitochondria (1%, 2% and 2% respectively). The resistant glyoxylate and DNA repair mutants, *cit2*, *icl1*, *mls1*, and *ogg1* had 6%, 20%, 27% and 26% of yeast cells with normal mitochondria after 15 minutes of SK-03-92 treatment, respectively.

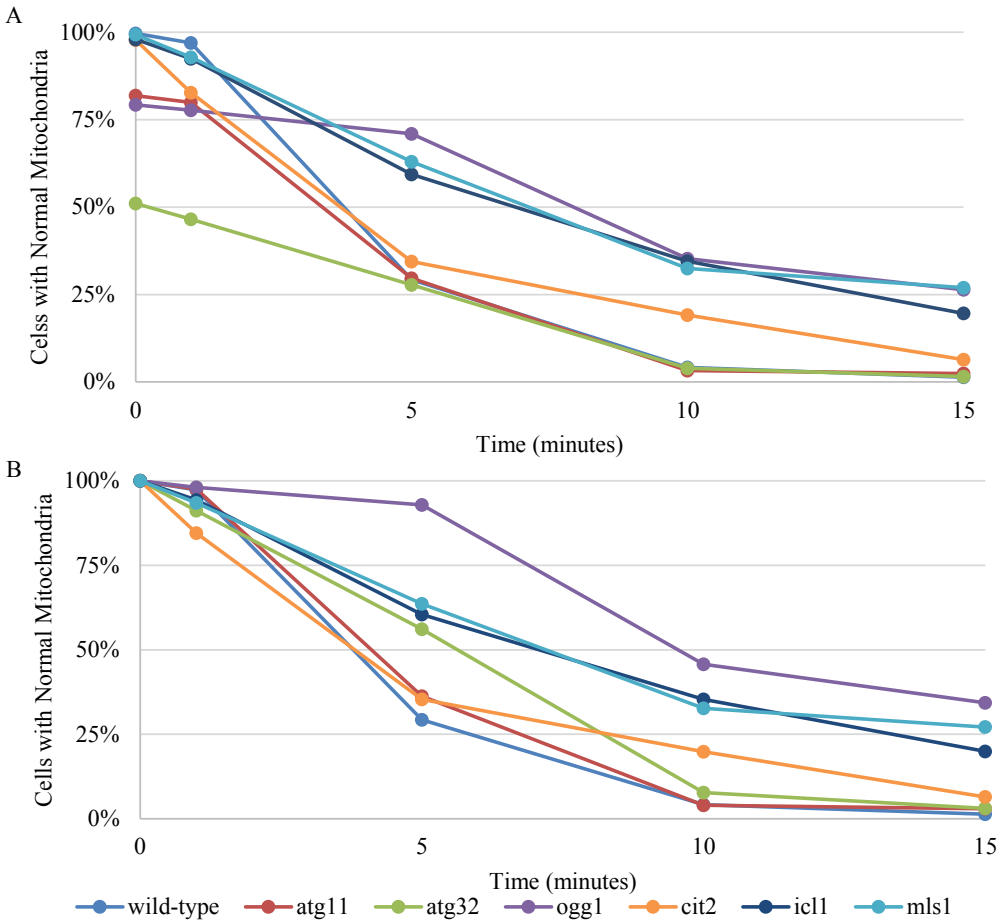

FIG. 9. Percentage of yeast cells with normal mitochondria over time after treatment with SK-03-92. (A) Raw data for yeast strains and (B) the same data for panel A normalized to DMSO controls. At least 100 cells were counted for each timepoint.

Because even untreated mutants had defective mitochondria, the data from FIG. 9A were normalized to the untreated control set at 100% normal mitochondria and logistic regression was performed between each mutant and wild-type yeast (FIG. 9B). Using these normalized data, all strains treated with SK-03-92 had nearly half as many cells with normal mitochondria within five minutes of treatment, with the exception of the mitochondrial DNA repair mutant *ogg1*, which took 10 minutes of treatment to reduce the number of cells with normal mitochondria to half (FIG. 9 B). The proportion

of cells with normal mitochondria remained constant beyond 15 minutes for each strain tested (data not shown). Mitophagy mutants (*atg11* and *atg32*) and wild-type cells had the greatest frequency of cells with mitochondrial abnormalities. Wild-type had <1% of cells with normal mitochondria after 15 minutes of treatment with SK-03-92. The mitophagy mutants, *atg11* and *atg32*, had 4% and 3% of cells with normal mitochondria after 15 minutes of treatment with SK-03-92, respectively (FIG. 9B). The glyoxylate mutants showed varying degrees of cells with abnormal mitochondria after SK-03-92 treatment. The *cit2*, *icl1*, and *mls1* mutants had 7%, 21% and 27% cells with normal mitochondria, respectively, after 15 minutes of treatment with SK-03-92 (FIG. 9B). The mitochondrial DNA repair mutant *ogg1* retained the largest proportion of cells with normal mitochondria after 15 minutes of treatment with SK-03-92, at 34% of cells (FIG. 9B).

Yeast Cell Death is Consistent with Mitochondrial Abnormalities

The percentage of *atg11*and *atg32* cells with normal mitochondria was higher than wild-type despite that these mutants were more sensitive to the lethal effects of SK-03-92 than wild-type as shown by a spot assay (FIG 2). To explore this discrepancy, a FungaLight live/dead kit was used as a second way to measure death of wild-type and the mutant yeast strains after treatment with SK-03-92. The green Syto 9 fluorochrome can permeate both live and dead yeast cells, but the red propidium iodide stain only permeates dead yeast cells when cell membranes are compromised. Yeast cells were categorized as propidium iodide negative if only green fluorescence was found throughout the cell or if only the cell periphery was red. Yeast cells that fluoresced green without any other amount of red fluorescence within the cell were considered propidium

iodide positive. A logistical regression was used to compare viability of mutants and wild-type cells.

All yeast strains tested remained highly viable (nearly 90% propidium iodide negative) after 30 minutes of SK-03-92 treatment. The fastest rate of death was observed in the wild-type strain, with 60% of cells dead after one hour and 91% of cells dead after four hours of treatment with SK-03-92 (FIG. 10). (Viability of cells remained constant for all strains after four hours of treatment, data not shown). Similar to wild-type, 40% of the *atg11* cells were dead after one hour and 85% of *atg11* cells were dead after four hours of treatment with SK-03-92 (FIG. 10). In contrast the *atg32* mutant remained quite viable with only 41% of cells dead after four hours of treatment with SK-03-92 (FIG. 10), despite being susceptible to mitochondrial damage and the most susceptible to SK-03-92 lethality as shown by prior spot assay experiments (FIG. 2A). Unexpectedly, the *ogg1* mutant showed the third highest death of all strains tested even though it had been the most resistant to mitochondrial abnormalities. Death of the yeast mitochondria DNA repair *ogg1* mutant was like that of *atg11*, with 32% of cells dead after the first hour and 84% of cells dead after four hours of treatment with SK-03-92 (FIG. 10). The death observed in the glyoxylate mutants, *cit2*, *icl1*, and *mls1*, was consistent with their resistance to mitochondrial abnormalities, with 74%, 68%, and 25% of the cells dead, respectively, after four hours of treatment with SK-03-92 (FIG. 10).

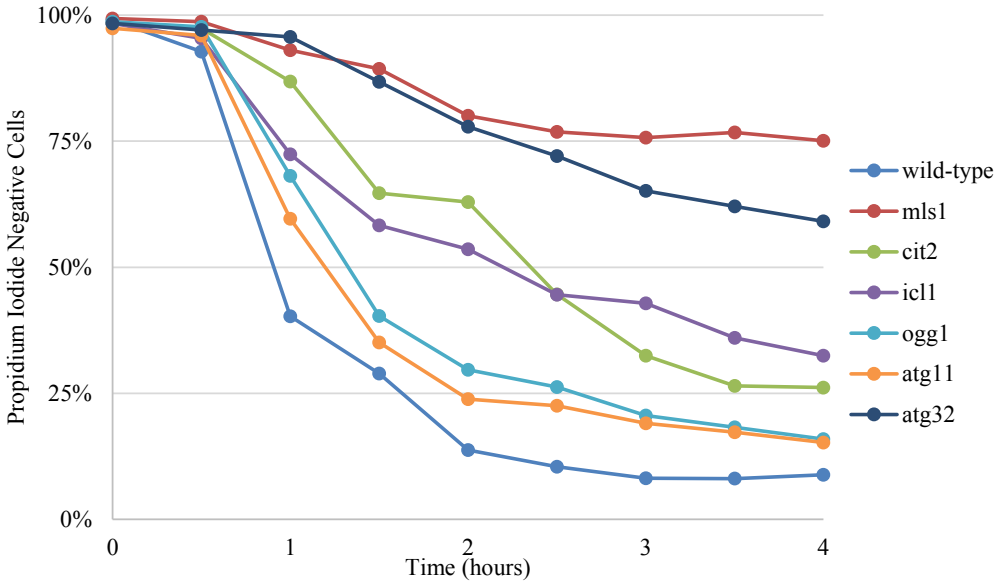

FIG. 10. Percentage of propidium iodide negative yeast cells over time after treatment with SK-03-92. Propidium iodide negative indicates cell viability. At least 300 cells were counted at each timepoint.

Cell Cycle Arrest and Synchronization Eliminates the Lethal Effects of SK-03-92

Because of the variation in viability of treated cells observed using live/dead staining versus other methods of measuring of viability such as the spot assay, experiments were designed to explore if phase of the cell cycle altered the effectiveness of SK-03-92, since yeast cells were not synchronized prior to treatment. Studies of other compounds have shown that treatment can have different degrees of effectiveness on cells depending on their stage of the cell cycle (47).

The cell cycle experiment was performed in two different ways. In one version, wild-type cells were arrested at G1, G1/S, or G2/M phase using standard methods (57), and then treated with SK-03-92 while arrested. Alternatively, yeast cells were arrested in G1, G1/S, or G2/M phase, then released to allow progression of the cell cycle as a synchronized population. The newly released yeast cells were immediately treated with SK-03-92. In both arrested and synchronized yeast, SK-03-92 treated yeast cells were

resistant in comparison to asynchronous cells regardless of the phase of the cell cycle the yeast cells were arrested (FIG. 11 and data not shown). Although arrested and synchronized cultures did show susceptibility to SK-03-92 after 24 hours of treatment (data not shown), cultures were likely asynchronous well before 24 hours because synchronized cultures typically only remain synchronized for the first 3-5 replication cycles after release from arresting compounds (57).

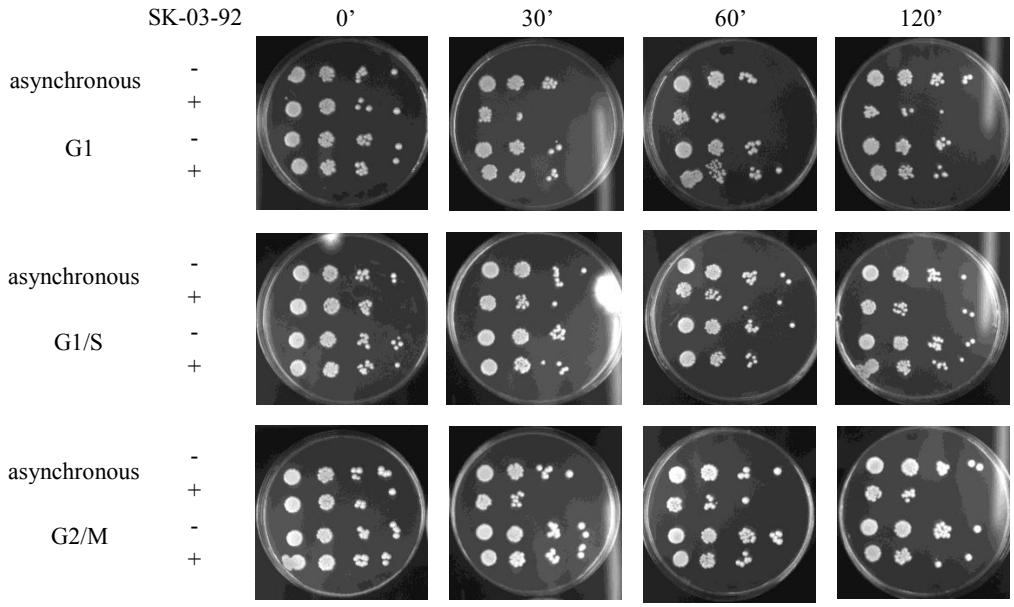

FIG. 11. Spot assays of asynchronous and synchronized wild-type yeast cells. Wild-type yeast cultures were treated with 8 µg/mL SK-03-92 (+) or an equal volume of DMSO (-) after being synchronized in G1, G1/S, or G2/M phase, or grown asynchronously. Samples were diluted and plated after 0’, 30’, 60’, and 120’ as described (Materials and Methods).

Light Microscopy Shows Variable Morphological Responses in SK-03-92 Treated THP-1 Cells

Microscopy techniques used to analyze yeast were also used to observe THP-1 cells. During preliminary work, THP-1 cells treated with SK-03-92 were observed to have various morphological responses, many similar to those elicited by yeast.

Morphological responses by THP-1 cells included normal (FIG. 12A, 12B), cells with phase bright inclusions (FIG. 12C, 12D), blebbing cells (FIG. 12E, 12F), blistering cells (FIG. 12G, 12H), pitted cells (FIG. 12I), “beads on a string” (FIG. 12J, 12K) (57), and the observation of extracellular debris fields (FIG. 12L). From a purely observational standpoint the morphological responses of THP-1 cells to SK-03-92 appeared to occur at different frequencies depending on the time after treatment and the final concentration of SK-03-92 treatment. However, also as with yeast, no morphological changes appeared to be directly related to cell death (data not shown).

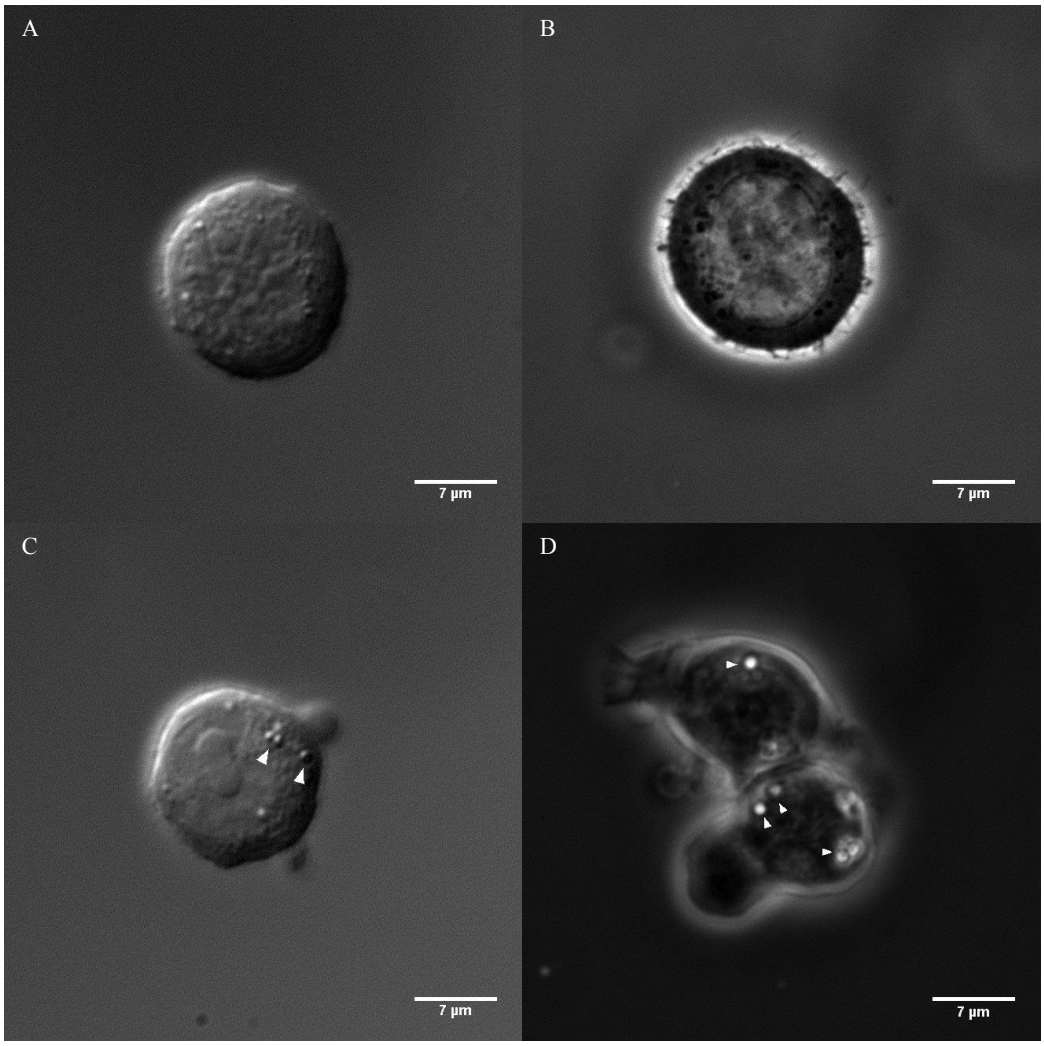

FIG. 12. Representative images of responses observed in THP-1 cells treated with SK-03-92 as described (Materials and Methods). (A, B) Normal THP-1 cells. (C, D) Treated cells displayed phase bright inclusions (arrow head), (E, F) blebs (arrow head), (G, H) blistering (arrow head in G), (I) pits, (J, K) beads on a string, (L) and debris fields.

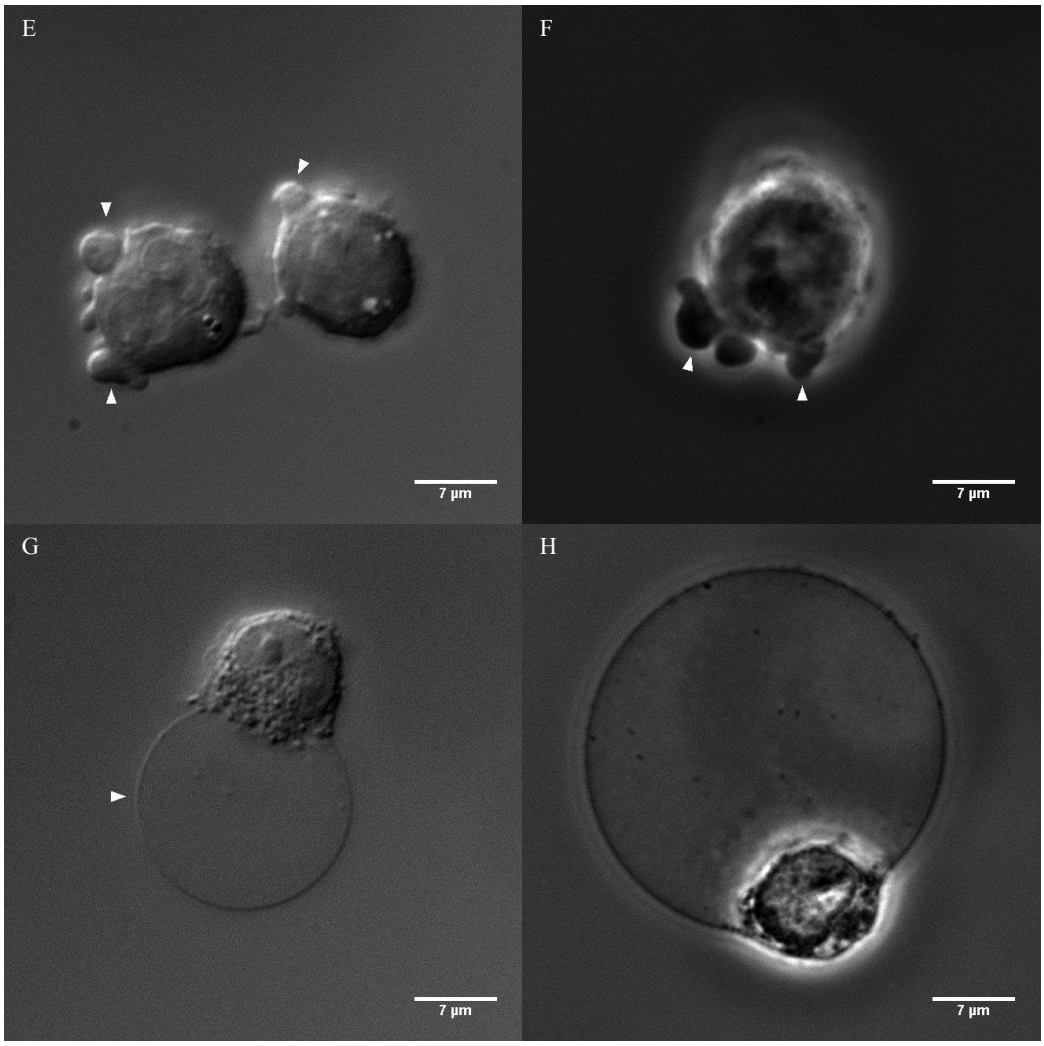

FIG. 12 - *continued*. Representative images of responses observed in THP-1 cells treated with SK-03-92 as described (Materials and Methods). (A, B) Normal THP-1 cells. (C, D) Treated cells displayed phase bright inclusions (arrow head), (E, F) blebs (arrow head), (G, H) blistering (arrow head in G), (I) pits, (J, K) beads on a string, (L) and debris fields.

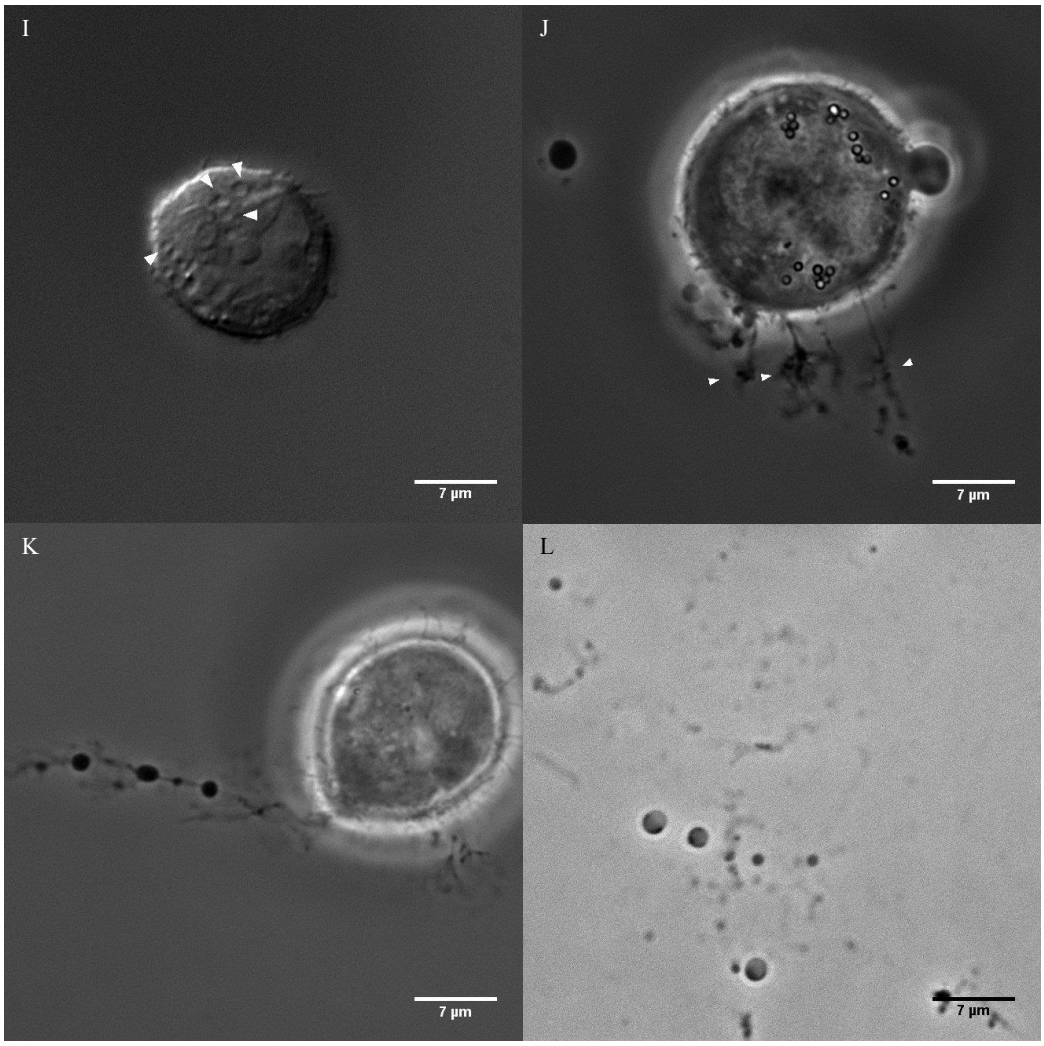

FIG. 12 - *continued*. Representative images of responses observed in THP-1 cells treated with SK-03-92 as described (Materials and Methods). (A, B) Normal THP-1 cells. (C, D) Treated cells displayed phase bright inclusions (arrow head), (E, F) blebs (arrow head), (G, H) blistering (arrow head in G), (I) pits, (J, K) beads on a string, (L) and debris fields.

THP-1 Mitochondria Show Increased Abnormities as Concentration of SK-03-92 Increases

Because yeast cells showed mitochondrial changes in response to SK-03-92, mitochondrial morphology was also examined in THP-1 cells. Abnormal morphological subgroups were easily distinguishable due to the larger size of the THP-1 cells as

compared to yeast cells. Unlike yeast mitochondrial networks, normal THP-1 mitochondrial networks appear speckled and are evenly distributed throughout the cytoplasm (FIG. 13A). The mitochondria of THP-1 cells treated with SK-03-92 showed two separate and distinct morphological responses, punctate or diffuse. The abnormal subgroup punctate appeared as spherical aggregates of mitochondria that were larger than the rod-like speckles of a normal network (FIG. 13B). The diffuse subgroup was like that of yeast with the cell having regions stained red (FIG. 13C). An early stage of diffuse mitochondria consisted of mitochondria appearing as ring-like structures rather than rod-like speckles (FIG. 13C). This ring-like response was categorized as diffuse because further observations showed that such cells progressed to diffuse mitochondria. Other observations included mitochondrial debris fields (FIG. 13D), and beads on a string morphology sometimes contained fluorescence, albeit too faint to produce images (data not shown).

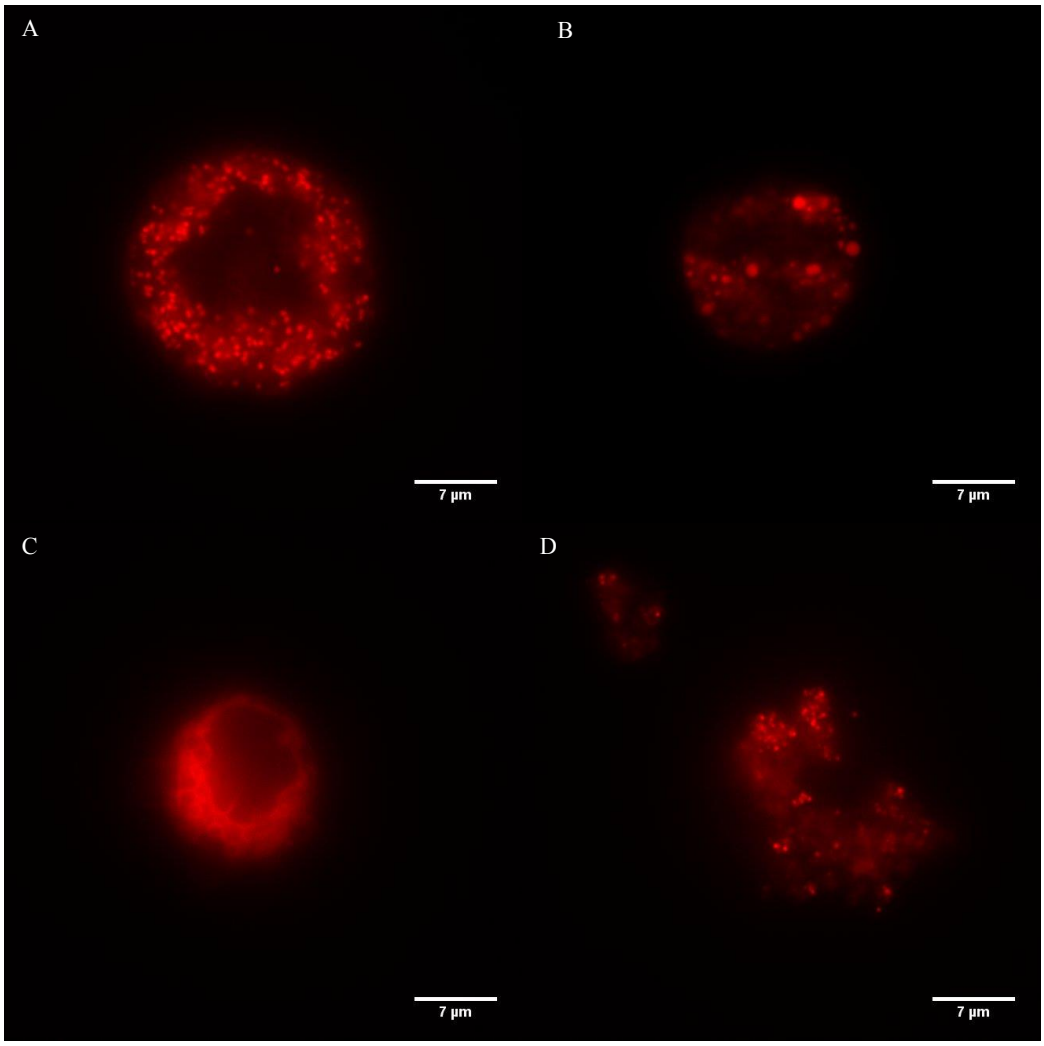

FIG. 13. Representative images of mitochondria of THP-1 cells treated with SK-03-92. (A) Normal mitochondria appeared as rod-like speckles around the outer periphery of the cell. Abnormal mitochondrial networks displayed two subgroups: (B) abnormal punctate and (C) abnormal diffuse. (D) Extracellular mitochondrial debris fields that stained red were also observed.

All concentrations of SK-03-92 led to mitochondrial morphological changes within the first five minutes of treatment with SK-03-92 (FIG. 12A). However, the percentage of THP-1 cells with abnormal mitochondria was proportional to the concentration of SK-03-92 used. After two hours of treatment with SK-03-92, 19% of cells showed abnormal mitochondria at 0 µg/mL SK-03-92, 60% of cells had abnormal

mitochondria at 5 μg/mL SK-03-92, 72% of cells had abnormal mitochondria at 10 μg/mL SK-03-92, 88% of cells had abnormal mitochondria at 15 μg/mL SK-03-92, 94% of cells with abnormal mitochondria at 20 μg/mL SK-03-92 and 97% of cells had abnormal mitochondria at 25 μg/mL SK-03-92 (FIG. 14A). After two hours of treatment with SK-03-92, the number of cells with abnormal mitochondria remained constant (data not shown).

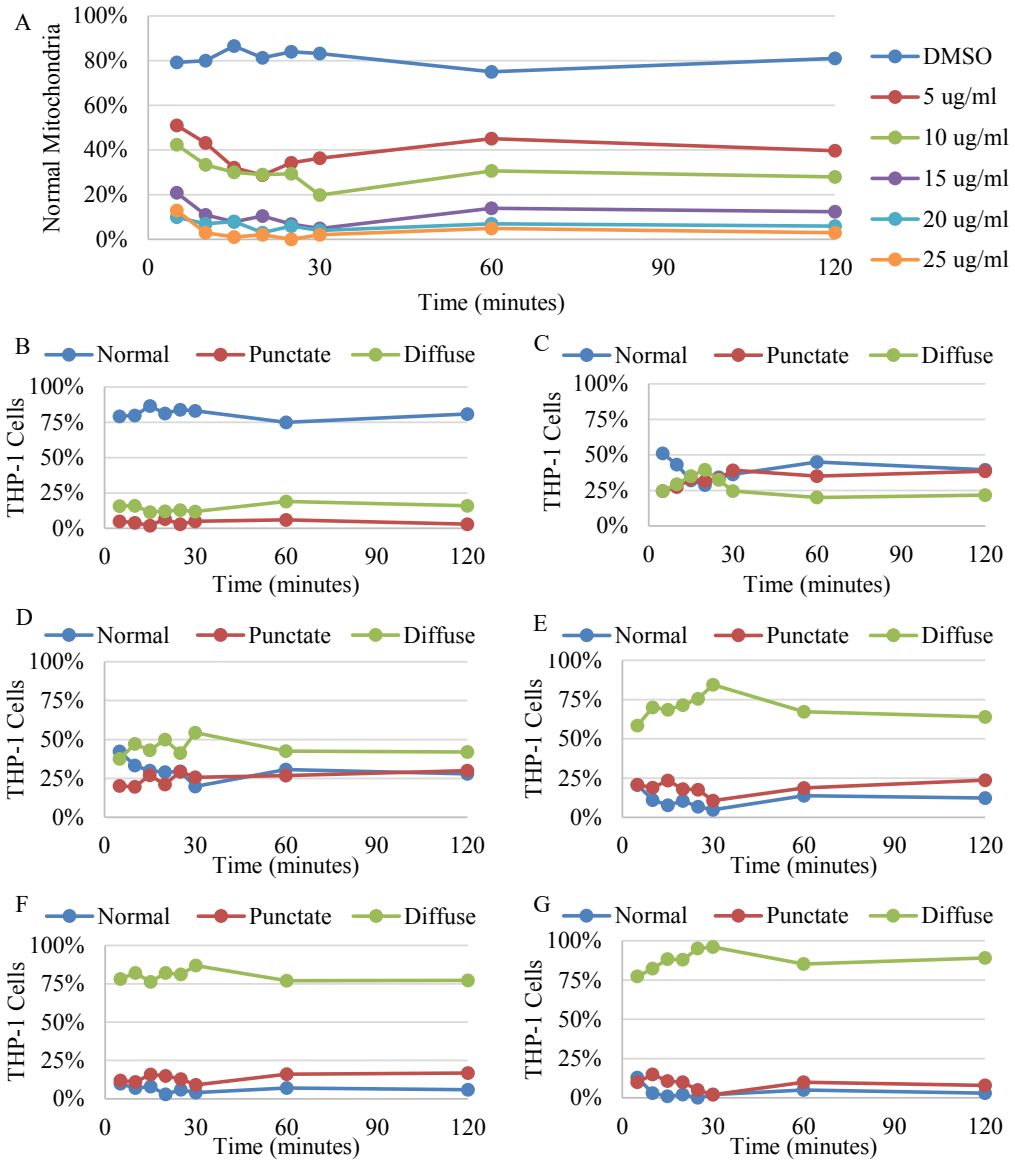

FIG. 14. Percentage of THP-1 cells with normal, punctate, or diffuse mitochondria over time after treatment with SK-03-92. THP-1 cells were treated with varying concentrations of SK-03-92, stained with MitoTracker Red CMXRos, visualized by fluorescence microscopy, and categorized as normal or one of two abnormal types, punctate or diffuse as shown in FIG. 13. (A) Percent of THP-1 cells with normal mitochondria after being treated with various concentrations of SK-03-92. (B) Percent of untreated (DMSO) THP-1 cells with normal, punctate or diffuse mitochondria. (C) Percent of THP-1 cells with normal, punctate, or diffuse mitochondria after treatment with 5 µg/mL SK-03-92. (D) Percent of THP-1 cells with normal, punctate, or diffuse mitochondria after treatment with 10 µg/mL SK-03-92. (E) Percent of THP-1 cells with normal, punctate, or diffuse mitochondria after treatment with 15 µg/mL SK-03-92. (F) Percent of THP-1 cells with normal, punctate, or diffuse mitochondria after treatment with 20 µg/mL SK-03-92. (G) Percent of THP-1 cells with normal, punctate, or diffuse mitochondria after treatment with 25 µg/mL SK-03-92.

The diffuse mitochondrial subgroup appeared to have a direct relationship with increasing concentration of SK-03-92, whereas the punctate mitochondrial subgroup appeared to have an inverse relationship with increasing SK-03-92 concentration (FIG. 14B). The highest percentage of cells that with punctate mitochondria and lowest percentage of cells with diffuse mitochondria were observed from SK-03-92 treatment at the lowest concentration (5 μg/mL) (FIG. 14B). As the concentration of SK-03-92 increased, the proportion of cells with the diffuse mitochondrial morphology increased after two hours of treatment, with 21% at 5 μg/mL, 42% at 10 μg/mL, 63% at 15 μg/mL, 78% at 20 μg/mL, and 90% at 25 μg/mL of SK-03-92 (FIG. 14B). The opposite was true for cells with the punctate mitochondrial morphology, with 38% of cells showing punctate mitochondria at 5 μg/mL of SK-03-92, 30% of cells at 10 μg/mL, 23% of cells at 15 μg/mL, 17% of cells at 20 μg/mL, and 8% of cells at 25 μg/mL of SK-03-92 after two hours of treatment (FIG. 14B).

THP-1 Death Correlates with Increased SK-03-92 Concentration

To examine THP-1 cell death in response to SK-03-92, a FITC Annexin V kit was used. The inversion of the phosphatidylserine is a hallmark feature of apoptotic cells (26). When an inversion of the phosphatidylserine occurs, FITC Annexin V binds to the phosphatidylserine and the THP-1 cell fluoresces green. When the cell membrane becomes compromised as in a necrotic cell, propidium iodide permeates the cell, staining the nucleic acids red. THP-1 cells that fluoresce both green and red are likely in late stage cell death, allowing both fluorochromes to bind in the THP-1 cell. THP-1 cells that were categorized as viable were negative for both red and green fluorescence (note that treated cells fluoresced blue, presumably due to the fluorescence properties of SK-03-92).

As expected, untreated control THP-1 cells were negative for both FITC Annexin V and propidium iodide, with 97% viable cells observed for the first eight hours, declining to 94% viable cells after 24 hours (FIG. 15). The number of viable THP-1 cells decreased relatively steadily over 24 hours for treated cells at all concentrations of SK-03-92 used. Although not statistically significant, the type of death pathway appeared to change as SK-03-92 concentration increased. THP-1 cells treated with lower concentrations of SK-03-92 (5 μg/mL and 10 μg/mL) had more FITC Annexin V positive/propidium iodide negative cells indicating apoptosis, whereas cells treated with higher concentrations of SK-03-92 (20 μg/mL and 25 μg/mL) had more propidium iodide positive/FITC Annexin V negative cells indicating necrosis (FIG. 15). The middle concentration (15 μg/mL) of SK-03-92 led to approximately equal numbers of THP-1 cells that were FITC Annexin V positive/propidium iodide negative, and FITC Annexin V negative/propidium iodide positive, with apoptosis being slightly more dominant after eight hours of treatment, and necrosis slightly more dominant after 24 hours of treatment. Numbers of THP-1 cells that were positive for both propidium iodide and FITC Annexin V generally increased as SK-03-92 concentration increased (FIG. 15).

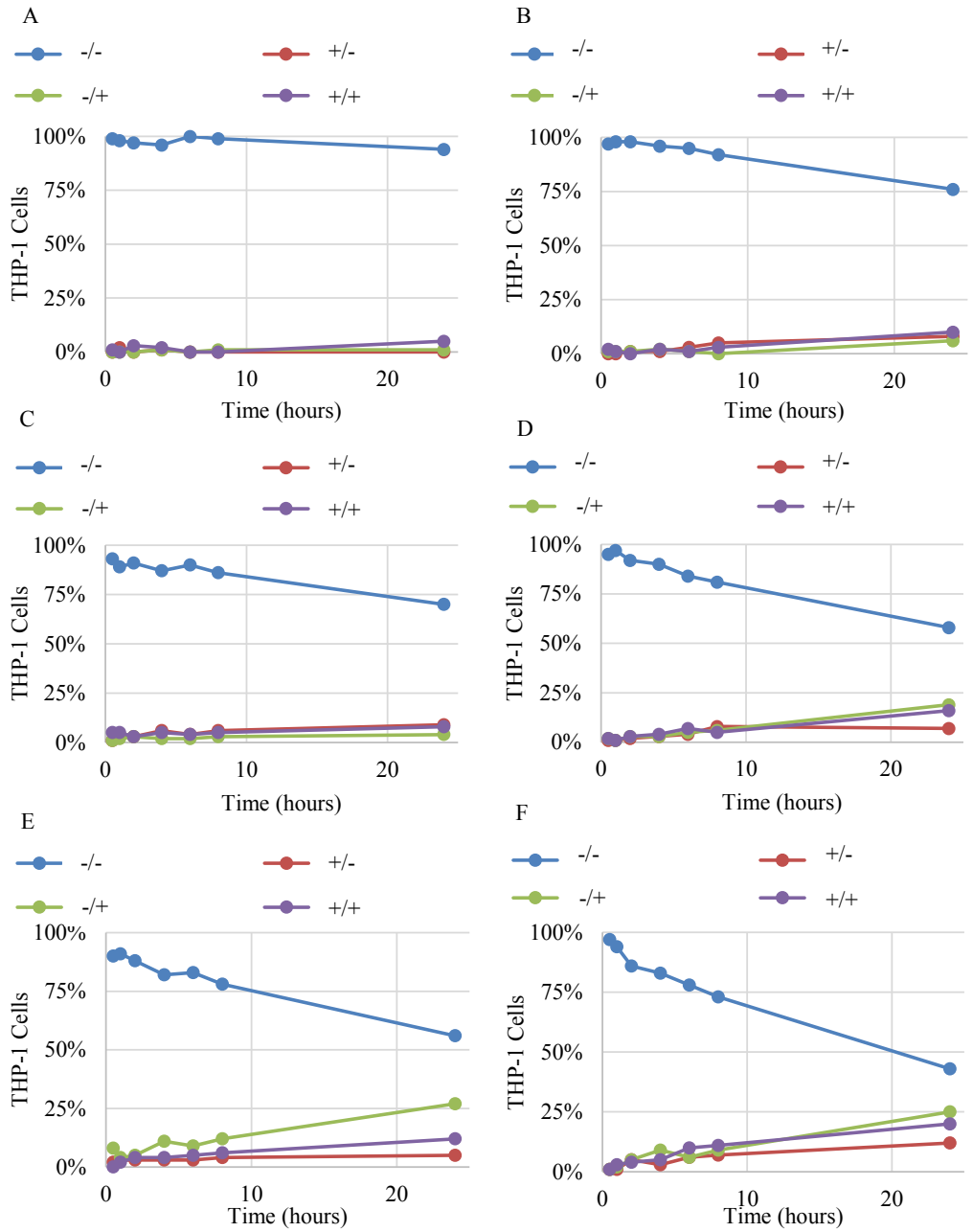

FIG. 15. Analysis of viability of THP-1 cells after treatment with SK-03-92 over time. THP-1 cells were treated with either (A) no SK-03-92 (DMSO), (B) 5 µg/mL SK-03-92, (C) 10 µg/mL SK-03-92, (D) 15 µg/mL SK-03-92, (E) 20 µg/mL SK-03-92, or (F) 25 µg/mL SK-03-92. Cells were stained with the FITC Annexin V kit to determine the percent of cells negative for each fluorochrome (-/-) indicating viable cells, positive for FITC Annexin V only (+/-) indicating apoptotic cells, positive for propidium iodide only (-/+) indicating necrotic cells, or positive for both FITC Annexin V and propidium iodide (+/+) indicating cells in late stage death.

DISCUSSION

Morphological Responses

The morphological changes observed in SK-03-92 treated wild-type yeast cells followed a general sequence of events over time. The data suggest that wild-type cells begin their response to SK-03-92 by inducing autophagy and/or mitophagy pathways, possibly to remove damaged organelles. MitoTracker Red CMXRos stained mitochondria were observed inside the vacuoles of treated yeast cells. The vacuoles also contained non-staining contents, which are likely other damaged cell components sent to the vacuole for autophagic processing. To identify these non-mitochondrial cell components, specific staining for a variety of cell components would be needed. Based on the sequence of morphological responses, it appears that after a period of processing, the vacuole contents are either degraded or moved out of the vacuole as phase bright inclusions. The phase bright inclusions are then moved to the cell membrane and released from the cell, possibly resulting in an abnormal cell wall and/or pits. Because the quantity of cells with pits remained relatively constant after one hour of SK-03-92 treatment, it is possible that the pit morphology is associated with the successful release of the phase bright inclusions, and once released, the pit morphology reverts to a normal morphology as quickly as new pits are formed. The presence of extracellular debris stained with mitochondrial stains also supports a model that SK-03-92 is leading to cells undergoing mitophagy and/or mitoptosis. Interestingly, none of these morphological responses

correlated with cell death and are likely indirect responses to the effects of stressors such as SK-03-92.

Mitophagy is Vital for Cell Survival After SK-03-92 Exposure

After the work on quantification of morphological responses in yeast had already been completed, a survival assay of wild-type yeast cells was performed outside of this study to determine the lethality of SK-03-92 on yeast shortly after treatment. Cells were treated with SK-03-92 and samples plated in ten minute intervals. Plates were incubated and colony forming units were counted to determine cell survival. Over 90% of wild-type yeast cells were killed by SK-03-92 within the first ten minutes of treatment using this assay (FIG. 16). The quick death influenced the remainder of this yeast study to focus on

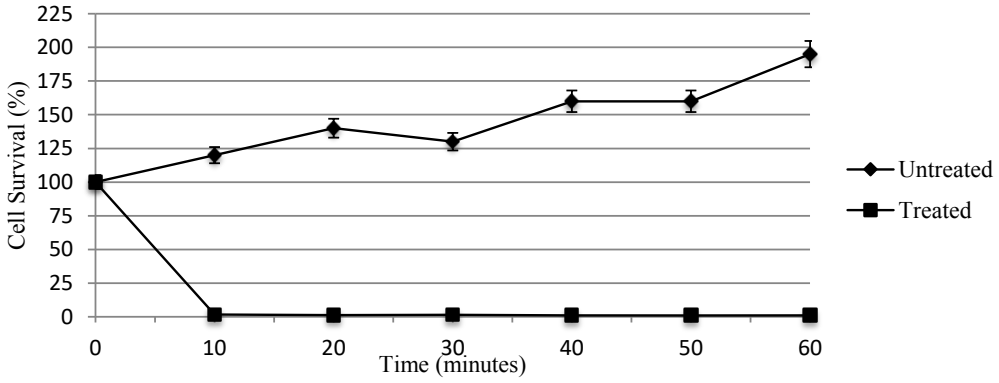

FIG. 16. Survival curve of wild-type yeast cells after treatment with SK-03-92. Yeast cells were treated with 8 µg/mL SK-03-92 (treated) or an equal volume of DMSO (untreated) as described (Materials and Methods). Cells were diluted after various times of treatment and plated to enumerate the number of colony forming units (A. Galbraith, unpublished data).

timepoints closer to treatment.

Previous work in the Galbraith lab had implicated mitochondria in the killing effects of SK-03-92. Previous experiments also showed that anaerobic and petite yeast cells which ferment, and stationary phase yeast cells which are not metabolically active,

were almost completely resistant to the lethality of SK-03-92. In addition, two mitophagy mutants, *atg32* and *atg11*, that wouldn't be able to rid cells of damaged mitochondria, appeared to die more readily than wild-type cells when treated with SK-03-92.

The data from the live/dead staining experiments showed *atg32* to be the second most resistant strain to SK-03-92 lethality (FIG. 10) despite that the *atg32* mutant was far more sensitive to SK-03-92 than other strains, including wild-type, by a spot plate assay (FIG. 2). Observations during the live/dead experiment for *atg32* suggested that many of the cells may have lysed, with fewer cells and more extracellular debris observed. Because the live/dead kit cannot quantify the number of lysed cells, this approach to measuring viability may have underestimated the number of dead cells by missing the lysed cells. To test this explanation, the concentrations of treated *atg32* mutant yeast cells over time can be determined using a hemocytometer to see if the cell concentration decreases over time.

Glyoxylate Mutants Resist Effects of SK-03-92

A fully functioning glyoxylate cycle may also contribute to mitochondrial damage since all the glyoxylate mutants (*cit2*, *icl1*, *mls1*) had less mitochondrial damage than wild-type cells, and showed less susceptibility to lethality by SK-03-92 then wild-type, *atg11*, and *atg32* yeast cells by both the plating assay (FIG. 2) and the live/dead experiment (FIG. 10).

Altogether, these data support a hypothesis that SK-03-92 causes mitochondrial damage. A potential explanation for the apparent general resistance of glyoxylate mutants to the effects of SK-03-92 on both mitochondria and viability is that a defective glyoxylate cycle reduces the amount of gluconeogenesis, biosynthesis, and most

importantly, leads to a decrease in overall metabolic activity of the yeast cell. The reduction of gluconeogenesis and biosynthesis would reduce the mitochondrial activity, potentially limiting SK-03-92 effectiveness. This hypothesis of a reduction in cell activity was further supported by results from previous experiments in which the addition of a fermentable carbon source (glucose) was shown to reduce the lethality of SK-03-92 when cells had the option of fermenting. Although gluconeogenesis would result in a fermentable carbon source, the energy cost to produce glucose from intermediates would be too great for fermentation to be a viable option, and therefore yeast cells would likely respire.

Mitochondrial DNA Repair Mutant Resists Mitochondrial Damage, but Not Death

The *ogg1* mutant showed the most resistance to the lethal effects of SK-03-92 (data not shown) and an initial delay in mitochondrial damage compared to all other mutants tested, suggesting that the inability to repair oxidative DNA damage is beneficial to the survival of SK-03-92 treated cells. The phenomenon does not appear to be a general characteristic of repair mutants because *rad50*, a repair mutant that cannot fix double strand breaks in nuclear DNA (58), appears to be as susceptible to SK-03-92 as wild-type yeast by our plating assay (data not shown). However, *msh1*, a mutant defective in repairing mitochondrial DNA damage like *ogg1*, is resistant to the killing effects of SK-03-92 by our plating assay (data not shown). It is counterintuitive that mutants defective in mitochondrial DNA repair would be more resistant to mitochondria damage by SK-03-92 than a wild-type strain. However, *ogg1* (and *msh1*) mutant yeast cells which cannot repair mitochondrial DNA damage may have always had to survive despite greater mitochondrial damage, perhaps eliciting other cellular functions to deal

with this damage. Another possible explanation is that, with an intact mitophagy process, the *ogg1* (and *msh1*) mutants have fewer functional mitochondria, and are therefore less metabolically active than wild-type cells. This could be tested by observing the quantity of mitochondria in wild-type versus mitophagy and mitochondrial DNA repair mutants. In addition, an *atg32* and *ogg1* double mutant would likely show more mitochondrial damage than a wild-type strain because the double mutant would not be able to fix damage or use mitophagy to eliminate the damaged mitochondria. It would be expected that the *atg32* and *ogg1* double mutant would have the greatest susceptibility to SK-03-92 observed thus far.

Arrested and Synchronized Cultures Show No Kill Effects of SK-03-92

Although arrested yeast cultures appeared unaffected by SK-03-92 treatment, it is not logical to conclude that all points in the cell cycle are resistant to SK-03-92. A better explanation is that the arrested cultures have reduced or no metabolic activity. As for the cells that were synchronized, they were not allowed the required two hour grow-out period before treatment (Materials and Methods) to ensure that the cells did not lose synchrony. If technically possible, yeast cultures should be synchronized again, and allowed the required two hour grow-out period, to see if this affects the response of the yeast cells to SK-03-92.

THP-1 Mitochondrial Abnormalities and Cell Death

Morphological changes were also observed in THP-1 cells in response to treatment with SK-03-92. However, only mitochondrial abnormalities were examined carefully. Death of THP-1 cells appeared to have a direct relationship with abnormal mitochondria because cell death increased with an increase in mitochondrial

abnormalities. With increasing concentration of SK-03-92, the percentage of THP-1 cells with the diffuse mitochondrial subgroup increased along with the number of propidium iodide positive cells (inviable) indicating necrosis. Necrosis has been shown to lead to the swelling of mitochondria, which would explain why diffuse mitochondria and propidium iodide positive THP-1 cells increased together (24). THP-1 cells with the punctate mitochondria subgroup correlated with THP-1 cells that were FITC Annexin V positive (indicating apoptotic cells), with both being inversely related to SK-03-92 concentration. The punctate mitochondria subgroup could be an indication of the re-localization of damaged mitochondria during an autophagy/mitophagy response, which would explain the correlation with FITC Annexin V positive apoptotic cells (43). Overall, observations of THP-1 cells further supported the hypothesis that the mitochondria are an important target of SK-03-92.

One observation of note is that there were more THP-1 cells with mitochondrial abnormalities than dead cells, suggesting that these mitochondrial abnormalities are not always fatal, and that THP-1 cells may be able to recover. If timepoints were taken later than 24 hours, perhaps more of these cells with abnormal mitochondria would have died. In support of this idea, previous experiments with THP-1 cells have shown that the number of live cells continues to decrease at higher concentrations of SK-03-92 for up to three days (FIG. 12 and data not shown).

SK-03-92 Lethality in THP-1 Cells is Dependent on Metabolic Activity

To further determine the requirement of metabolic activity and the effectiveness of kill by SK-03-92, THP-1 cells were diluted into refrigerated media before treatment, rather than pre-warmed media, to reduce metabolic activity. Death of THP-1 cells after

SK-03-92 treatment was reduced by about 20% in cold media (data not shown), although death still increased with increased drug concentration. The death of THP-1 cells observed at high concentrations of SK-03-92 may explain results seen when testing the efficacy of SK-03-92 in a mouse model infected with *S. aureus* (20). Low concentrations of SK-03-92 would not be able to kill *S. aureus* or immune cells, whereas an intermediate concentration of SK-03-92 would be sufficient to kill *S. aureus*, but not immune cells, as immune cells are larger and not as metabolically active as bacteria. High concentrations of SK-03-92 may result in death of bacteria, but could act as a toxin to immune cells. With the death of immune cells in the mouse cell, persister bacteria cells could repopulate in the mouse without being cleared by the immune system. At extremely high concentrations of SK-03-92, it is reasonable to believe that SK-03-92 would become toxic to most cells, including non-immune host cells. Non-immune host cells are, in most cases, less metabolically active than immune cells.

The observation that a multicellular organism such as a mouse does not show systemic effects of SK-03-92 suggests that SK-03-92 may only be effective against single celled organisms or cells that behave as a single cell, an intriguing idea that needs further research. One way to approach this would be to examine the effects of SK-03-92 on other multicellular organisms as well as other eukaryotic cell lines.

Final Summary

Prior to this work the Galbraith lab had learned that yeast mutants that cannot eliminate damaged mitochondria by mitophagy, *atg11* and *atg32*, are more sensitive to the killing effects of SK-03-92 than wild-type yeast, indicating a possible mitochondrial target for SK-03-92. Other than the exceptions observed with the *ogg1* and *atg32* yeast

mutants, the proportion of cells with mitochondrial abnormalities from SK-03-92 treatment did, in fact, correlate with cell death for all yeast strains tested and THP-1 cells treated with various concentrations of SK-03-92. The mitochondrial abnormalities are worth further pursuit as a possible cause of death for the collection of observations made so far. It also appears that a functioning glyoxylate cycle increases mitochondria damage and lethality of SK-03-92. The increase in susceptibility to SK-03-92 of yeast cells with a functioning glyoxylate cycle was supported by the glyoxylate yeast mutants, *cit2*, *icl1,* and *mls1*, showing the lowest percentage of cells with mitochondrial abnormalities and the highest resistance to the lethal effects of SK-03-92 in comparison to wild-type, *atg11*, and *atg32* strains.

Future experiments should include investigation of the interactions of SK-03-92 with the mitochondria. This could involve analyzing more yeast mutants related to mitochondrial function, or use of a variety of stains that detect varying properties of the mitochondria and its products. The glyoxylate cycle should be investigated further as well. Investigation of the glyoxylate cycle could be done by visualizing the peroxisomes of wild-type and glyoxylate mutant yeast cells with stains that detect damage and abnormalities to determine if the glyoxylate cycle is also a target of SK-03-92. The conflicting results among *atg32*, *atg11* and *ogg1* strains regarding viability and its relationship to mitochondrial abnormalities should also be investigated further. It is possible that the appearance of higher sensitivity to SK-03-92 on plates is due to a phenomenon known as “viable but not culturable”, a phenomenon that has been observed in bacteria (59). The mitochondrial abnormalities may not be lethal to some individual cells, but may prevent them from being able to reproduce to form a colony on a plate.

Further research on the effects of SK-03-92 on THP-1 cells could include a more detailed analysis of mitochondria with the same stains used in this work. It would also be useful to treat a variety of other eukaryotic cell lines with SK-03-92 to determine if the responses seen in THP-1 cells are universal or specific to THP-1 cells.

With future exploration, SK-03-92 could still serve as a potential antimicrobial for many pathogenic single-celled organisms to aid in the race against antimicrobial resistant organisms. If other human cell lines are shown to be unaffected by SK-03-92 this would increase the applicability of SK-03-92 as an antimicrobial for humans.

REFERENCES

1. **Yoneyama H, Katsumata, R.** 2006. Antibiotic resistance in bacteria and its future for novel antibiotic development. Biosci Biotechnol Biochem **70**:1060-1075.

2. **Ochman H, Lawrence JG, Grolsman EA.** 2000. Lateral gene transfer and the nature of bacterial innovation. Nature. **405**:299-304.

3. **Martinez JL, Baquero F.** 2000. Mutation frequencies and antibiotic resistance. Antimicrob Agents Chemother. **44**:1771-1777.

4. **Neu HC.** 1992. The crisis in antibiotic resistance. Science. **5073:**1064-1073.

5. **Lin J, Nishino K, Roberts MC, Tolmasky M, Aminov RI, Zhang L.** 2015. Mechanisms of antibiotic resistance. Front Microbiol **6:**34.

6. **Centers for Disease Control and Prevention.** 2013. Antibiotic resistance threats in the United States, 2013. Centers for Disease Control and Prevention, Atlanta, GA.

7. **Baquero F, Blazquez J.** 1997. Evoultion of antibiotic resistance. Trends Ecol Evolut. **12**:482-487.

8. **Vergis EN, Hayden MK, Chow JW, Snydman DR, Zervos MJ, Linden PK, Wagener MM, Schmitt B, Muder RR.** 2001. Determinants of vancomycin resistance and mortality rates in *Enterococcal* bacteremia. Ann Intern Med. **405**:484-492.

9. **Klein E, Smith DL, Laxminarayan R.** 2007. Hospitalizations and deaths caused by methicillin-resistant *Staphylococcus aureus* United States, 1999-2005. Emerg Infect Dis. **13**:1840-1846.

10. **Spelberg B, Powers JH, Brass EP, Miller LG, Edwards E.** 2003. Trends in antimicrobial drug development: implications for the future. Clin Infect Dis **38**:1279-1286.

11. **Butler MS, Buss AD.** 2006. Natural products – the future scaffolds for novel antibiotics? Biochem Pharmacol. **71**: 919-929.

12. **Clardy J, Fischbach MA, Currie CR.** 2009. The natural history of antibiotics. Curr Biol. **19**:R437-R441.

13. **Lam KS**. 2007. New aspects of natural products in drug discovery. Trends in Microbiol. **15**:279-289.

14. **Xiao K, Zhang HJ, Xuan LJ, Zhang J, Xu YM, Bai DL**. 2008. Stilbenoids: chemistry and bioactivities. Stud Nat Prod Chem **34**:453–646.

15. **de la lastra CA, Villegas I.** 2005. Resveratrol as an anti-inflammatory and anti-aging: mechanisms and clinical implications. Mol Nutr Food Res. **5:**405-430.

16. **Baxter RA.** 2008. Anti-aging properties of resveratrol: review and report of a potent new antioxidant skin care formulation. J Cosmet Dermatol. **7**:2-7.

17. **Paulo L, Ferreira S, Gallardo E, Queiroz J, Domingues F.** 2010. Antimicrobial activity and effects of resveratrol on human pathogenic bacteria. Worl Microbiol Biotechol. **26:**1533.

18. **Kabir MS, Engelbrecht K, Polanowski R, Krueger SM, Ignasiak R, Rott M, Schwan WR, Stemper ME, Reed KD, Sherman D, Cook JM, Monte A.** 2008. Bioorg Med Chem Let. **18**:5745-5749.

19. **Schwan WR, Kabir MS, Kallaus M, Krueger S, Monte A, Cook JM.** 2012. Synthesis and minimum inhibitory concentrations of SK-03-92 against *Staphylococcus aureus* and other gram-positive bacteria. J Infect Chemother. **18**:124–126.

20. **Schwan WR, Kolesar JM, Kabir MS, Elder EJ, Williams JB, Minerath R, Cook JM, Witzigamann CM, Monte A, Flaherty.** 2015. Pharmacokinetic/toxicity properties of the new anti-staphylococcal lead compound SK-03-92. Antibiotics. **4:**617-626.

21. **Saraste A, Pulkki K.** 2000. Morphologic and biochemical hallmarks of apoptosis. Cardiovasc Res. **3:**528-537.

22. **Zong WX, Thompson CB.** 2006. Necrotic death as a cell fate. Genes and Dev. **20:**1-15.

23. **Edinger AL, Thompson CB.** 2004. Death by design: apoptosis, necrosis and autophagy. Curr Opin Cell Bio. **6:**663-669.

24. **Galluzzi L, Kroemer G.** 2008. Necroptosis a specialized pathway of programmed necrosis. Cell. **7:**1161:1163.

25. **Krysko DV, Vanden Berghe T, D'Herde K, Vandenabeele P.** 2008. Apoptosis and necrosis: detection, discrimination and phagocytosis. Method. **3:**205-2-21.

26. **Elmore S.** 2007. Apoptosis: a review of programmed cell death. Toxicolo Patho. **4:**495:516.

27. **Wang C, Youle RJ.** 2009. The role of mitochondria in apoptosis. Annu Rev Genet. **43:**95-118.

28. **Lewis K.** 2000. Programmed death in bacteria. Microbiol Mol Biol Rev. **3:**503-514.

29. **Keren I, Kaldalu N, Spoering A, Wang Y, Lewis K.** 2004. Persisters cells and tolerance to antimicrobials. FEMS Immunol Med Microbiol. **230**:13-18**.**

30. **Lewis K.** 2010. Persister cells. Annu Rev Microbiol. **64**:357-372.

31. **Lewis K.** 2007. Persister cells, dormancy and infectious disease. Nat Rev Microbiol.**1:**48-56.

32. **Edwards AM.** 2012. Phenotype switching is a natural consequence of *Staphylococcus aureus* replication. J. bacteriol. **194**:5404-5412.

33. **Lewis K.** 2007. Persister cells, dormancy and infectious disease. Nature. **5**:48-56.

34. **Engel SR, Dietrich FS, Fisk DG, Binkley G, Balakrishnan R, Costanzo MC, Dwight SS, Hitz BC, Karra K, Nash RS, Weng S, Wong ED, Lloyd P, Skrzpek MS, Miyasato SR, Simison M, Cherry M.** 2014. The reference genome sequence of Saccharomyces cerevisiae: then and now. G3. **3:**389-398.

35. **Botstein D, Fink GR.** 2011. Yeast: An experimental organism for 21st century biology. Genet. **189**:695-704.

36. **Saccharomyces Genome Database** http://www.yeastgenome.org

37. **Marsland PA.** 2014. Intracellular penetration of novel antimicrobials in human THP-1 macrophages infected with Listeria monocytogenes. UWL.

38. **Auwerx J.** 1991. The human leukemia cell line, THP-1: a multifaceted model for the study of monocyte-macrophage differentiation. Experientia. **47**:22-31.

39. **Greenhalf W, Stephan C, Chaudhuri B.** 1996. Role of mitochondria and C-terminal membrane anchor of Bcl-2 in Bax induced growth arrest and mortality in Saccharomyces cervisiae. FEBS let. **1-2:**169-175.

40. **Kanki T, Wang K, Cao Y, Baba M, Kilionsky DJ**. 2009. Atg32 is a mitochondrial protein that confers selectivity during mitophagy. Dev Cell. **17**:98-109.

41. **Okamoto K, Kondo-Okamato N, Ohsumi Y.** 2009. Mitochondria-anchored receptor Atg32 mediates degradation of mitochondria via selective autophagy. Dev Cell. **1:**87-97.

42. **Kanki T, Wang K, Cao Y, Baba M, Kilonsky DJ.** 2009. Atg32 is a mitochondrial protein that confers selectivity during mitophagy. Dev Cell. **1:**98-109.

43. **Lyamzaev KG, Nepryakhina OK, Saprunova, VB, Bakeeva LE, Pletjushkina OY, Chernyak BV, Skulachev VP.** 2008. Novel mechanism of malfunctioning mitochondria (mitoptosis): formation of mitoptotic bodies and extrusion of mitochondrial material from the cell. Biochim and Biophys Acta. **7-8:**817-825.

44. **Tinari A, Garogalo T, Sorice M, Esposti MD, Malorni W.** 2007. Mitoptois: different pathways for mitochondrial execution. Autophagy. **3:**282-284.

45. **Kunze M, Pracharoenwattana I, Smith SM, Hartig A.** 2006. A central role for the peroxisomal membrane in glyoxylate cycle function. BBA-Mol Cell Res. **1763**:1441-1452.

46. **Fernie AR, Carrari F, Sweetlove LJ.** 2004. Respiratory metabolism: glycolysis, the TCA cycle and mitochondrial electron transport. Curr Opin Plant Biol. **3:**254-261.

47. **White D, Drummond JT, Fuqua C.** 1995. The physiology and biochemistry of prokaryotes. New York: Oxford press. 214-219.

48. **Kozmin S, Slezak G, Reynaud-Angelin A, Elie C, de Rycke Y, Boiteux S, Sage E.** 2005. UVA radiation is highly mutagenic in cells that are unable to repair 7,8-dihydro-8-oxoguanine in Saccharomyces cerevisiae. Proc Natl Acad Sci. **102:**38.

49. **Pommier Y, Leo E, Zhang H, Marachand C.** 2010. DNA topoisomerases and their poisoning by anticancer and antibacterial drugs. Chem Biol. **5:**421-433.

50. **Guthrie F, Fink G.** 1991. Guide to yeast genetics and molecular biology. Method Enzymol. **194**:3-21.

51. **European Saccharomyces cerevisiae archive for functional analysis (Euroscarf)** http://www.uni-franfurt.de/fb15/mikro/euroscarf/index.html

52. Tsuchiya S, Yamabe M, Yamaguchi Y, Kobayashi Y, Konno T, Tada K. 2006. Establishment and characterization of a human acute monocytic leukemia cell line (THP-1). Int J Cancer. **26**:171-176.

53. Abramoff MD, Magalhaes PJ, Ram SJ. 2004. Image processing with imagej. Biophotonics. **11**:36-42.

54. Reggiori F, Klionsky DJ. 2013. Autophagic processes in yeast: mechanism, machinery and regulation. Gen. **194:**341-361.

55. Atkin-Smith GK, Tixeira R, Paone S, Mathivanan S, Collins C, Liem M, Goodal KJ, Ravichandran KS, Hulett MD, Poon KH. 2015. A novel mechanism of generating extracellular vesicles during apoptosis via a beads-on-a-string membrane structure. Nat. **6:**7439.

56. Shaw JM, Nunnari J. 2002. Mitochondrial dynamic and division in budding yeast. Trends Cell Biol. **12:**178-184.

57. Lieberman HG. 2004. Cell cycle checkpoint control protocols. Method Mol Biol. **241:**77-92.

58. Game JC, Mortimer RK. 1974. A genetic study of x-ray sensitive mutants in yeast. Mutat Res. **3:**281-292.

59. Oliver JD. 2005. The viable but nonculturable state in bacteria. J Microbiol.**43:**93-100